Article

Investigations on the Ethylene Polymerization with Bisarylimine Pyridine Iron (BIP) Catalysts

Elsa M. Schoeneberger and Gerrit A. Luinstra *

Institute for Technical and Macromolecular Chemistry, University of Hamburg, Bundesstr. 45, 20146 Hamburg, Germany; elsa.schoeneberger@chemie.uni-hamburg.de

* Correspondence: luinstra@chemie.uni-hamburg.de; Tel.: +49-40-42838-3162

Abstract: The kinetics and terminations of ethylene polymerization, mediated by five bisarylimine pyridine (BIP) iron dichloride precatalysts, and activated by large amounts of methyl aluminoxane (MAO) was studied. Narrow distributed paraffins from initially formed aluminum polymeryls and broader distributed 1-polyolefins and (bimodal) mixtures, thereof, were obtained after acidic workup. The main pathway of olefin formation is beta-hydrogen transfer to ethylene. The rate of polymerization in the initial phase is inversely proportional to the co-catalyst concentration for all pre-catalysts; a first-order dependence was found on ethylene and catalyst concentrations. The inhibition by aluminum alkyls is released to some extent in a second phase, which arises after the original methyl groups are transformed into n-alkyl entities and the aluminum polymeryls partly precipitate in the toluene medium. The catalysis is interpretable in a mechanism, wherein, the relative rate of chain shuttling, beta-hydrogen transfer and insertion of ethylene are determining the outcome. Beta-hydrogen transfer enables catalyst mobility, which leads to a (degenerate) chain growth of already precipitated aluminum alkyls. Stronger Lewis acidic centers of the single site catalysts, and those with smaller ligands, are more prone to yield 1-olefins and to undergo a faster reversible alkyl exchange between aluminum and iron.

Keywords: single site olefin polymerization; Cossee-Arlmann mechanism; kinetic study; beta-hydrogen transfer; chain shuttling; bisimine iron dichloride; MAO; aluminum alkyl; living olefin polymerization; ethylene oligomerization

1. Introduction

Plastics are an essential part of everyday life, in their preparation, and also in part, due to the diverse options of recycling profit from effective catalysts. This holds in particular true for polyolefins with a european annual output of 25 million tons. Polyethylene thereunder is the most important and worldwide most used plastic [1,2]. The overall property profiles of the various types of polyethylene make it indispensable for a manifold of short and long term applications. It is robust, electrically and thermal isolating, easy and cheap to process. Due to its high social, and thus, commercial relevance, even 60 years after the start of industrial PE-production, there are still efforts underway to optimize olefin polymerization [3]. These comprise the development and investigation of new catalysts in the context of morphology (powder) control, and the improvement of existing processes and technologies. The main targets are an extended control of the product and particle properties resulting in a reduction of the production costs and extension of the application profiles [4,5].

One extension of insights into the preparation of polyethylene of the last decades is on the action of late transition metal complexes as catalysts for the low-pressure ethylene-polymerization [4,6–19]. This class includes the iron (and cobalt) catalysts that were independently reported in the 1990s by Gibson [20,21] and Brookhart [22,23]. These typically consist of metal ions (e.g., iron) coordinated by a tridentate bisarylimine pyridine

ligand (BIP ligand) [24–26]. The vast development can be taken from several recent reviews [27–35] and from very recent publications and patents [36–51].

Effective BIP iron complexes are easily prepared from commercially available chemicals and easily handled, giving some advantages over the early transition metal complexes. Iron is also environmentally more benign than, e.g., chromium or vanadium. The oxidation state of the iron in active catalysts is not without debate, but here, the majority found formulation as iron(II) is used [52–54]. A significant body of literature and patents exemplify the interest and usefulness of the approach [4,55–60]. More complex ligand structures of symmetrical and unsymmetrical tridentate BIP ligands were developed in the course of time [39,44–47,49,51,57–66].

These ligands often comprise bulky substituents (e.g., dibenzo cycloheptyl or benzhydryl groups) at the ortho-position of the aniline aryl part and/or are carbocycle fused at the pyridine backbone. Such iron based catalysts bearing steric extended ligands often provide high activities and are remarkably thermostable in ethylene polymerizations [39,44,46,47,49,51,60–67]. A further stabilization can be reached by immobilizing the pre-catalysts on solid supports [50,67–69].

Depending on the ligand structure, different polymerization activities and products are obtained [20,37,44,49,60–62]. Linear polyethylene of high density and crystallinity is predominantly obtained as product from simple catalysts [25,26]. Oligomers of ethylene can effectively be prepared, using BIP Ligands with smaller aryl substituents [9,23,70]. The field of application of BIP iron based systems could additionally be extended for polymerizations of other monomers than ethylene, such as (cyclic) esters, dienes, vinyl monomers, and CO_2 [71,72].

Aluminum alkyls act as effective cocatalysts in the ethylene conversions, providing the anionic chain starter after a salt metathesis with the iron chloride entity [35,73,74]. They also convert the bisimine pyridine metal dichloro complexes into a for olefin polymerization active form. Typically, methyl aluminoxane (MAO), and modified derivatives (MMAO, MMAO-12) are used as the activating cocatalyst, but also other aluminum alkyls, like trimethyl, triethyl or triisobutyl aluminum (TMA, TEA and TIBA) are effective and act as cocatalyst and/or chain transfer agents [75–77]. In addition, a number of successful studies have been undertaken to transfer commercial accessible aluminum alkyls into alternative cocatalyst for the BIP type of iron catalysts [78,79]. A ligand-free, cationic species is expected when "theoretically pure" MAO is used as the cocatalyst [73,77,80–83]. The formation of bimetallic cationic structures by transfer of an $AlMe^{2+}$ end group from MAO to the catalyst under formation of $AlMe_3$ has also been proposed for forming the cationic iron complex [81,84,85]. The formation of the active catalyst is an equilibrium reaction with a dormant form, either with the coordination of an aluminate or with present excess of aluminum alkyls. The (re)coordination of the aluminum or aluminate alkyl will also result in a chain end transfer. The result is the formation of aluminum-terminated polymeryl chains as products (chain shuttling) [86–88].

The nature and formation of active sites is an important factor that influences the activity and the constitution of the products. The identity of the cocatalyst is important in that context [83,89,90]. Simple aluminum alkyls (TMA, TEA, TIBA) will interact more exothermic with the tentatively cationic catalyst center, resulting in the formation of hetero bimetallic species. The Lewis acid-base adducts were described several times [75–77,91–94]. Neutral heterobimetallic adducts may show an one electron reduction process with the ligand, leading to active or inactive catalysts [72,76,77,80,95].

The transformation of the bimetallic adducts into polymerization active catalyst can be detected in the presence of ethylene [80]. Some catalysts are not activated by TMA (or TEA), tentatively because of the quasi-irreversible formation of catalytically not active bimetallic Fe-Al species [90]. A complete deactivation by TMA with simultaneous formation of methane or extrusion of iron(0) has also been described in combination with the possibility of reactivation in the presence of MAO [96–99].
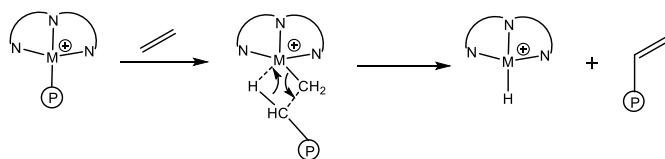
Chain termination in the ethylene polymerization, mediated by BIP catalysts of late transition metals, occurs by two major, parallel pathways. The common beta-hydrogen elimination leads to polyolefins (Scheme 1) [6,100]. The beta-hydrogen elimination may yield a metal hydride (Scheme 1, middle), or in the case of a transfer to a monomer, an ethyl catalyst derivative is obtained (Scheme 1, bottom). A chain end transfer to the cocatalyst by a transmetallation gives access to (cocatalyst) metal polymeryls [20,23,101,102]. The preparation of aluminum polymeryls is successful when the chain transfer to aluminum is the dominant termination mechanism (catalytic "Aufbau Reaktion") [88,103]. The aluminum polymeryls can subsequently be reacted with electrophilic agents, resulting in polar -end functionalized products. The aluminum polymeryl entities can, thus, be converted to aluminum alkoxides by oxidation with oxygen from air. Subsequent acidic work up yields hydroxyl-functionalized polyethylene [102–105].

We have developed an interest in the preparation of such terminal hydroxyl terminated polyethylenes for the preparation of blockcopolymers. These are compatible with polyethylene and can extend the property profile, e.g., by enhancing the surface energy. Attempts were, thus, undertaken to establish an easy to use procedure for their synthesis on a kg scale using BIP iron complexes. They yield highly active catalysts with cost effective commercial available aluminum alkyls or with the more expensive MAO [90,91,106].

Chain transfer to aluminum:
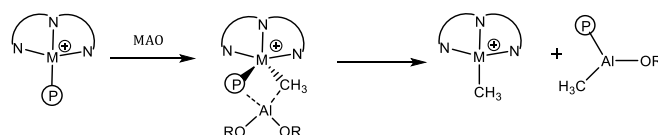
β-hydrogen elimination to metal:

β-hydrogen transfer to monomer:
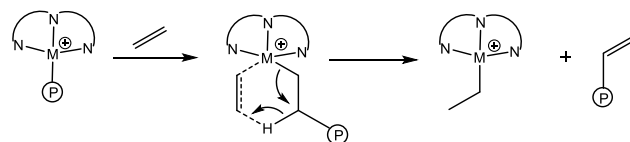
Scheme 1. Possible chain terminations in BIP iron catalyzed ethylene polymerization.

A comprehensive kinetic study with five derivatives (Scheme 2) was carried out with the objective to prepare paraffinic products with molecular weights in the range below 10 kDa. The kinetic study was also interesting in gaining insight into the type and relative rates of termination reactions as function of conversion [20].
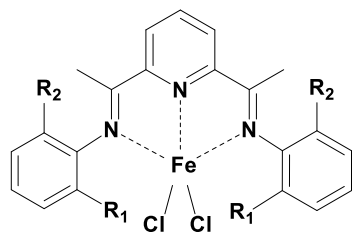
Scheme 2. Structures of the used bisarylimine pyridine iron precatalysts ($R_{1,2}$ in Table 1).

Table 1. Substitution pattern of the investigated catalysts **1–5**.

Catalyst	R_1	R_2
1	Cl	Cl
2	Et	Et
3	Me	Me
4	Me	Cl
5	H	Me

The outcome of ethylene polymerization with BIP iron catalysts will be influenced by several interdependent factors, like the ligand structure of the catalyst, the activation mechanism, the nature and concentration of the cocatalytic aluminum alkyls and the termination mechanism. The catalysts are chosen to get information separately on electronics, methyl and chloride substituents are about of the same size (complexes **1**, **3**, **4**) and sterics (complexes **5**, **3**, **2**). These catalysts are not unknown, in fact a larger body of literature on their catalytic action is available [4,20–23,107–116]. The actions of catalyst **3** activated by MMAO and TIBA, e.g., was reported to give bimodal polyethylenes [20,22,70,114–116]. A multisite activity of **1** was concluded on the basis of the time dependent product formation also using ^{14}C labeling, and a deconvolution of the size exclusion chromatographic traces [107,114]. The catalyst **5** and MMAO systems, on the other hand, react with ethylene to yield 1-olefins with a Flory-Schulz distribution [23,78]. This is a typical result of the process involving irreversible growth and termination reactions.

The published data preclude a direct assessment of the action of the various catalytic systems to be conducted at comparable conditions, such as temperature, cocatalyst(s), concentrations, ethylene pressure and dosing, as well as reaction times span quite a range. The Al/Fe ratios, e.g., are found between 2000–5000 [4,20,23,47,60,79,82]. It is particularly important to note that the catalytic "Aufbau Reaktion" changes the aluminum (or zinc based) alkyl cocatalysts [90,117,118]. The observations of the catalytic action should encompass the (time dependent) system of catalyst and cocatalyst. This should also include the state of aggregation. Mostly toluene is used as a solvent, which is not particularly capable of keeping the product polymers (olefins and aluminum polymeryls) in solution (up to about 1500 Da) [90,117]. It must, thus, not be a surprise that a complex situation results that may appear confusing.

The present kinetic study is conducted on similar systems of catalysts and cocatalyst and under conditions of a moderate ethylene uptake. Long lasting and constant polymerization rates could be achieved. The amount/concentration of cocatalyst is varied in a broad range, partly with an Al/Fe ratio as high as 75,000. These conditions are favorable for a target of preparing aluminum polymeryls of tunable length. The moderate rate of ethylene polymerization enables the change in aluminum alkyls to be observed and to address the heterogeneity of the reaction medium. A simple mechanistic picture arises with a single site catalyst, and this action is readily interpretable in terms of rate and products within a set of three elementary reactions. The insights of the kinetic study were also useful in the context of safety issues, with the target of running the polymerization in 10 and 50 L equipment. In addition, the route to minimizing the unwanted β-hydrogen elimination as a termination step became clear for their appropriate reaction conditions and catalyst structure [6,78,102–105,119]. The target of low molecular weight products, at a low rate (for temperature control), was also a chance to study the insertion polymerization without larger diffusion limitations.

2. Results

2.1. Polymerization System

The ethylene polymerizations were carried out as solution polymerizations in absolute toluene in 1 L steel reactors at ethylene partial pressures of 1 to 3.5 bar. The catalyst system is built by the injection of the BIP iron dichloride pre-catalyst as toluene suspension into the reaction medium containing the co-catalyst and after saturation with ethylene. Most of the

reactions were carried out as semi-batch processes at a constant ethylene pressures with a continuous flow of ethylene. The internal pressure, temperature and the resulting ethylene volume flow (in mL/min) was monitored and recorded. The isobaric reaction control during semi-batch polymerizations leads to a fairly constant monomer concentration in the reaction medium. The reactions were carried out at 5–15 °C with μmol concentrations of the catalysts. The rate of the polymerization can then be hold a range that allows the temperature to be kept constant. The heat of reaction is removed by cooling of the reactor wall. The ethylene volume flow provides information on the current and average rate of the chain growth reaction, as long as ethylene diffusion is not rate limiting (which was the case). The ethylene concentration is proportional to the partial pressure of the ethylene, and Henry's law is valid in the range of pressure used (Supplementary Material). Monomer consumption is found dependent on the applied ethylene partial pressure concomitant with the concentration in solution. The decay of pressure after closing the feeding line, which turns to a batch system, was also used to monitor the consumption. The preceding period of semi-batch operation ensured an almost complete activation of the pre-catalyst (vide infra).

Not all of the pre-catalysts immediately become active catalysts or become active all the time. Activation takes some time and includes dissolution under alkylation of the sparingly soluble pre-catalysts. Deactivation comprises reversible reactions to dormant species and decomposition normally occurs (which was always minor in these set of experiments) [77,80,96–99,120]. Therefore, the measured values for the activity are the product of the insertion rate in the active catalyst(s) and its concentration. The true activity of a catalyst, in the sense of propagation rate, is hard to assess and structure-activity relationships need to be interpreted with appropriate care (Section 3).

A preliminary set of experiments with several cocatalysts could provide one further insight [121,122]. The pre-catalysts **1**–**5** can be activated for ethylene polymerization by various aluminum alkyls, which also act as chain transfer agents (CTAs) [74,82,83,123,124]. The average activities over the first 30 minutes is dependent on the cocatalyst concentration. Increasing the cocatalyst concentration will eventually lead to less active systems. Catalysts generated from **2** and **3** showed high activities with trimethyl aluminum (TMA) or triethyl aluminum (TEA) as activator. In contrast, catalyst **1** with dichloro substituted aniline ligands could not sufficiently be activated by those (Figure 1; in the following, no distinction will be made in the notation of the precatalyst and the derived active catalyst). The more electron deficient complex **1** seems to coordinate aluminum compounds to a larger extent. The formation of a free coordination site for ethylene does not seem to occur. Methyl aluminoxane (MAO) and triisobutyl aluminum (TIBA) activate all pre-catalysts for ethylene polymerization with sufficient activity, MAO giving the highest level (Figure 1). The coordinating power of the aluminum compounds is important for the (initial) activity.
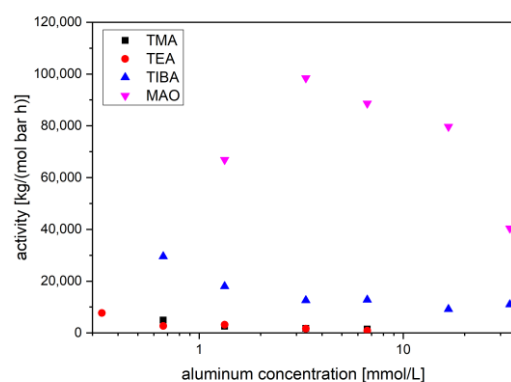

Figure 1. Average activity of catalyst **1** during the first 30 min, depending on the log aluminum concentration for various cocatalysts at 0.6 μmol/L of **1**, 15 °C and 1 bar of ethylene pressure.

2.2. Kinetics

A kinetic study was performed using commercially available MAO solutions from one batch with an assumed constant concentration of MAO and TMA. MAO contained residues of TMA from which it is prepared [125]. MAO builts an active system with all pre-catalysts. It also gave the most long-lasting activity, perhaps indicating that a reactivation of an irreversible deactivated alkyl catalyst species can occur. Polymerization of ethylene in toluene solutions, with high MAO concentrations, proceeded for several hours. The course of the polymerization activity was characterized by an initial period of increasing rate as the catalyst became active. The increase in rate appeared to proceed along an intermediate stage (Figure 2a, Figures S3–S6) before the maximum was reached. The slope of the initial reaction rate increase was steeper when less MAO was used. A pre-equilibrium of inactive bimetallic species and active catalyst would explain the observed behavior. Also, the time span between the second and first stage depended on the MAO concentration, i.e., the more MAO is present, the longer the period and the flatter the slope after reaching the first turning point. This is the consequence of the transformation of its methyl groups to longer alkyls, and it took longer the more MAO was present (vide infra). Higher alkyls coordinate less strongly (c.f. TIBA), and thus, the activity increased if the initially present MAO was increasingly transformed into alkyl aluminoxane (AOA) and the TMA to higher aluminum alkyls [90]. This behavior was observed for all catalysts, and is thus, interpreted as a cocatalyst effect.

This initial period was followed by a second period of almost constant activity (maximum activity) and subsequently by a decay in two steps. The latter is only substantial in the time span of observation at lower aluminum concentrations (Figure 2a). The period of maximum activity was sustained mostly over the residual period of experiments at higher MAO concentrations, i.e., except for a smaller decline that varied to some degree in the experiments. The ethylene massflow of an experiment with catalyst **3** with 17 mmol/L MAO, e.g., showed an earlier decrease in the maximum reaction rate. Such variations were also observed in other experiments (Figures S3–S6). These observations were interpreted as fluctuations of a sensitive reaction system. Local temperature fluctuations, diffusion barriers or the presence of small amounts of contamination can lead to the early decline of maximum rates. The maximum rates within a series of experiments is very reproducible and consistent (Table S1).The reaction mixtures become turbid in due course on account of the limited solubility of longer alkyl moieties in toluene. This will limit the mobility of the chains, the chain ends however will still be accessible to the catalyst (Section 3). This smaller decline is followed in experiments with the lowest MAO concentrations by a much faster loss of ethylene consumption. The origin of latter observation was not addressable, the usual explanation of appearing diffusion barriers or failing reactivation of inaccessible precipitated catalyst containing polymers may apply (Section 3) [126].

A full set of experiments was carried out with the objective to establish the rate law of propagation r_p (Equation (1)), defining that the variables are the monomer concentration [M], the precatalyst concentration [Fe] and the aluminum alkyl concentration [Al] and a k_{obs}, the observed rate constant (Equation (1); concentrations in mol/L). The rate at the first maximum/turning point in activity is inversely proportional to the MAO concentration (Figures 2a and 3a, Figures S3–S6). It most closely represents the concentration of the starting materials with known concentrations and species. The way of determination and the character of the inflection point is subjected to some scattering, leading to reactions orders close to minus one, i.e., in a range between -0.8 and -1.1 (Figure 3a; Table S1). The formation of a dormant catalyst by the coordination of changing aluminum alkyls is consistent with this observation (Supplementary Material). Observed lower rates at higher aluminum concentration can, thus, be understood [45,90].

The nearly constant maximum rate of ethylene uptake after activation is less dependent on the initial MAO concentration. The average activity became independent from the concentration of aluminum alkyls at higher concentrations (Figure 2b). The origin of this behavior may lie in the character of the transformed MAO solution itself, containing

Lewis acid and basic moieties that form equilibria too, and the precipitation of aluminum polymeryls. As a consequence, the concentration and the equilibrium constants for forming dormant species are no longer defined nor uniform:

$$r_{p,i} = -\frac{d[M]}{dt} = k_{obs}[M]^a[Fe]^b[Al]^c = k_{obs}\frac{[M][Fe]_0}{[Al]}\ [mol/L\ s]. \qquad (1)$$

It is further found that ethylene consumption by all of the catalyst systems has a first order dependence in the concentrations of ethylene and the pre-catalyst [114]. The rate of the chain propagation as function of the iron concentration was convincingly obtained from semi-batch experiments applying the method of flooding at higher MAO concentrations (Supplementary Material). The aluminum concentrations and the n-alkyl derivatives appeared to stay fairly constant in semi-batch reactions at maximum rate. The measured reaction rates were averaged over 10 min respectively after reaching the maximum rate, in order to obtain as precise data as possible regarding the kinetics of chain propagation (Figure S2). The maximum reaction rate equals the constant ethylene consumption. A double logarithmic plot of these rates and the iron concentration gives the reaction order as slope (Figure 3b). The slope has a gradient of one for all catalysts.
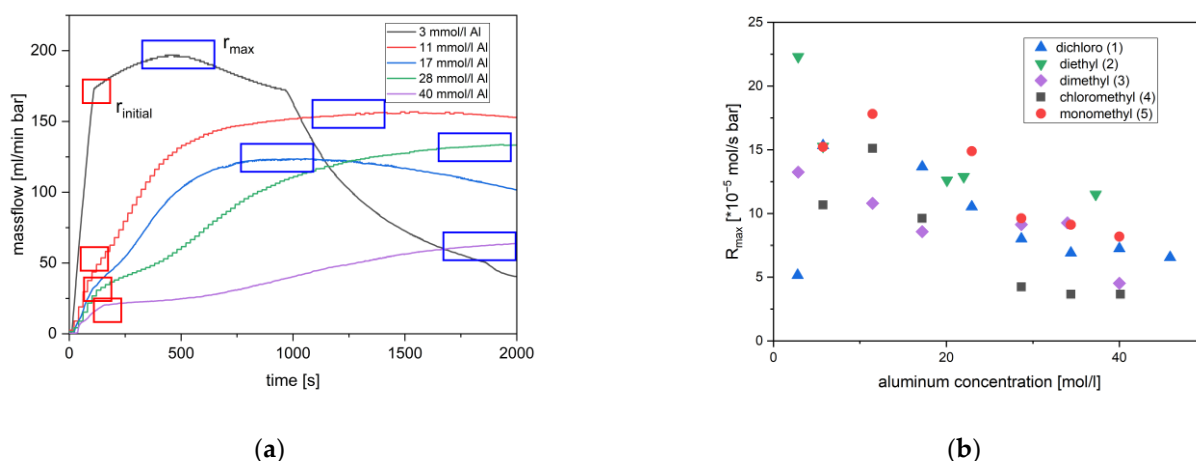

(a)　　　　　　　　　　　　　　　　　　　　　　　　(b)

Figure 2. (**a**) Ethylene massflow at varying aluminum concentrations during polymerization catalysis by **3** (other catalysts see Figures S3–S6). (**b**) Constant maximum reaction rate (normalized to 0.6 μmol/L catalyst) as a function of the aluminum concentration for catalyst **1–5**. Reaction conditions: 0.6 μmol/L catalyst **1**, **2** and **3**, 0.8 μmol/l catalyst **4**, 0.55 μmol/L catalyst **5**, 10 °C (15 °C for **1**), 2 bars of ethylene.

The reaction order with respect to ethylene was obtained in the pseudo-batch operation, interrupting the feed of ethylene and monitoring the decay of pressure in a small interval of time and pressure at the maximum ethylene take-up (Figure 3c). The decay follows a natural exponential function, a linear dependence of the $Ln(p)$ from the time is confirmed. The rate of pressure of ethylene was normalized to an iron concentration of 1 mol/L in order to make the catalysts quantitatively comparable (Figure 3c, Figures S4–S6; Table 2). It essentially gives the same data as in the experiments leading to Figure 3b, but with a higher accuracy with respect to the intercept at the *y*-axis. The data from semi-batch ethylene uptake and the batch pressure decline, thus, giving a consistent set. A rate constant $k'(= k_{obs}[Al]_t^{-1})$ can be extracted to rank the order of catalyst activities (Table 2, Figure S1). The values of k' decreases in the order $k'(\mathbf{2}) > k'(\mathbf{5}) > k'(\mathbf{3}) > k'(\mathbf{1}) > k'(\mathbf{4})$.

Table 2. Slopes k' of the regression lines of the logarithmic pressure-time plot (normalized to 1 mol/L catalyst concentration) at 10 °C and 40 mmol/L of Al at t = 0 (MAO).

Catalyst	k' [s^{-1}]
1	400 (650 [a])
2	1850
3	990
4	350
5	1360

[a]: at 15 °C, 45 mmol/L of MAO.

(**a**)

(**b**)

(**c**)
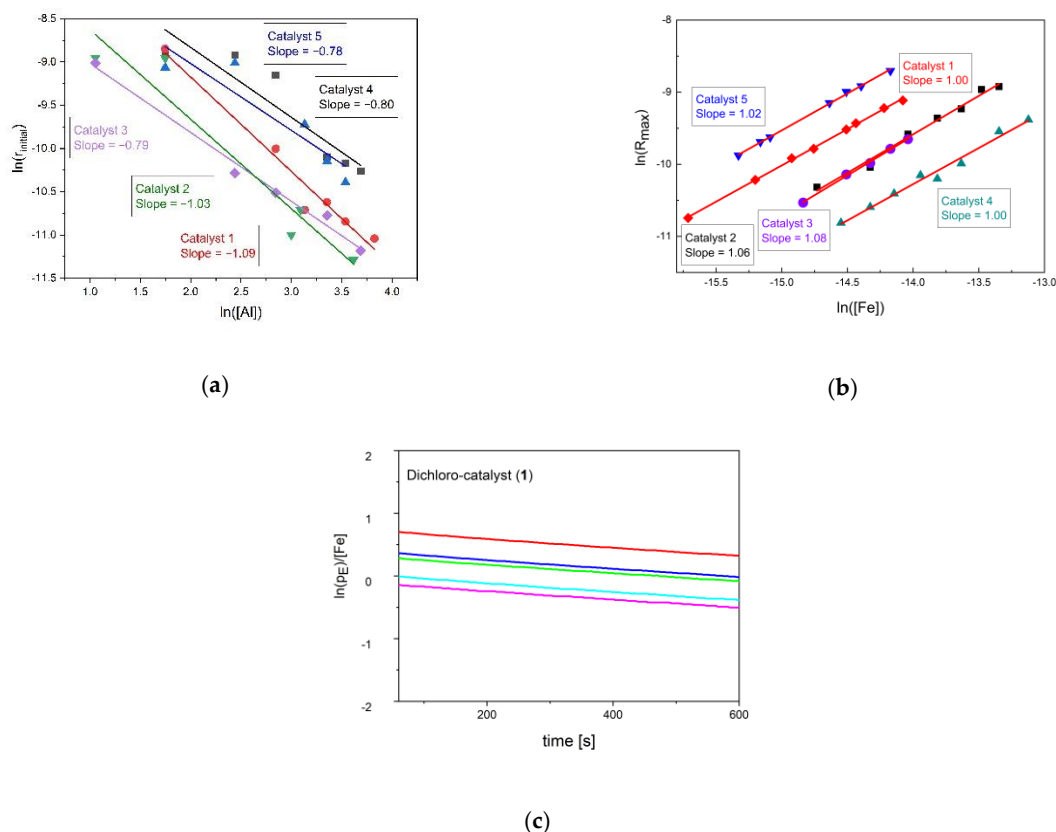
Figure 3. (**a**) Logarithmic plots of the initial reaction rate against the cocatalyst concentration for catalyst **1–5** (see Table S1 for confidence interval). Reaction conditions: 0.6 µmol/L catalyst **1,2** and **3**, 0.8 µmol/L catalyst **4**, 0.55 µmol/L catalyst **5**, 10 °C (15 °C for **1**), 2 bars of ethylene. (**b**) Logarithmic plots of the maximum reaction rate against the catalyst concentration for catalyst **1–5** (Table S1). Reaction conditions: 40 mmol/L Al (MAO) (45 mmol/L for **1**), 10 °C (15 °C for **1**), 2 bars of ethylene. (**c**) Normalized logarithmic ethylene pressure loss against the reaction time for catalyst **1** (data of other catalysts in Figures S7–S10). Reaction conditions: 0.7 µmol/L of catalyst, 45 mmol/L of Al (MAO), 15 °C, 1–3 bar of ethylene.

2.3. Calalytic Action and Product Properties

Activities are only one aspect in the context of the targeted aluminum polymeryls. The catalysts are highly active and productive, and would allow the product yield to be enhanced through prolonged times or higher concentrations. The products of the catalysis are at least of equal importance. The products obtained are highly linear with no branches detected in NMR spectra. 1-Olefins and aluminum polymeryls are obtained as a result of beta-hydrogen elimination in iron alkyls respectively of an alkyl group exchange between aluminum and iron (chain shuttling). The efficiency of starting a chain by a methyl group in MAO is variable, mostly below 20%. This may reflect the readily available alkyl entities in MAO related to aluminum trialkyls. The aluminum polymeryls will react during the quenching of the reaction mixture with ethanol/HCl/water mixture with protons and/or

oxygen (Figure 4). The hydrolysis gives linear paraffins. Oxidation by air oxygen during the workup may also partly in the presence of protons yield aluminum alkoxides, giving terminal hydroxy functionalized PE after hydrolysis [102]. However, these products were essentially absent in the product mixture. The catalyst alkyl concentration itself is too low to contribute to the ensemble of products.
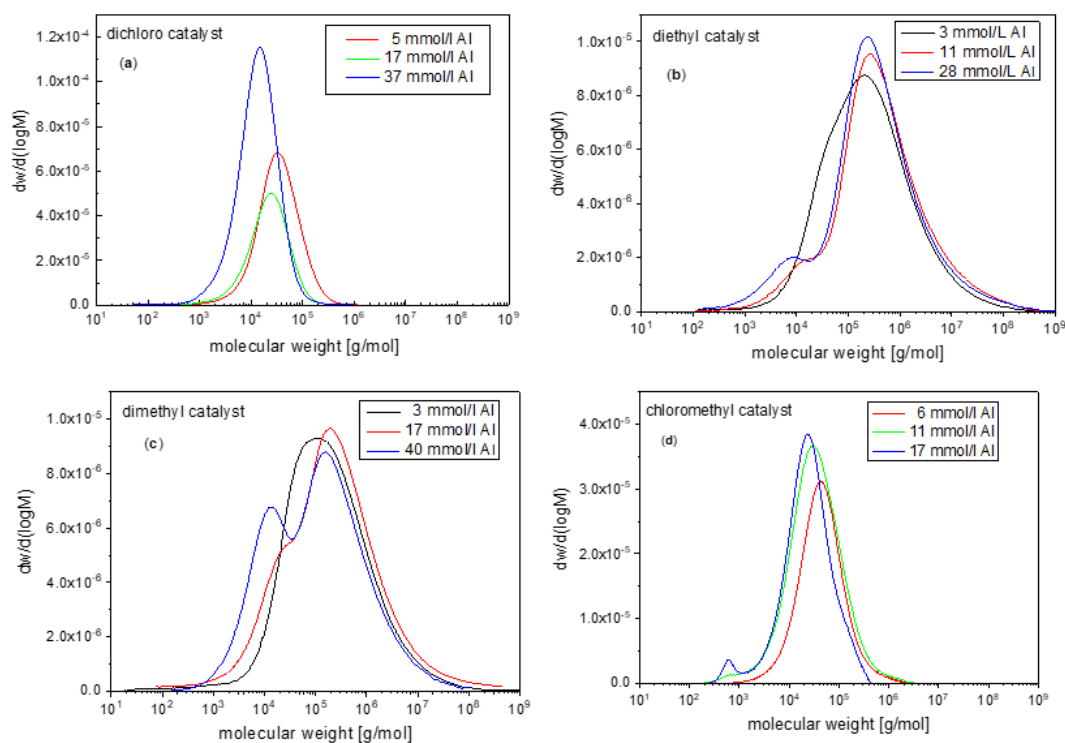

Figure 4. Molecular weight distribution of catalyst **1** (**a**), **2** (**b**) and **3** (**c**) and **4** (**d**) at various aluminum concentrations. Reaction conditions: 0.6–0.8 μmol/L catalyst, 10–15 °C, 2 bar of ethylene.

The molecular masses are as planned in the lower range. The masses were obtained from endgroup analyses in the proton NMR spectra and by SEC (Table 3). The values are mostly close to each other, however, both methods have a limited accuracy and differences occur. These originate from the inherent errors in determining the integral values of small signals of sparingly soluble compounds in NMR spectra. In addition, the linearity of the log M–elution volume dependency, especially at low molecular weights, peak selection and the validity of the Kuhn-Mark-Houwink-Sakurada equation for obtaining absolute masses in SEC determinations gives some spread.

The distribution of the molecular mass of the mixture of paraffines and olefins may be monomodal (with a shoulder) or bimodal and may span quite a range of polydispersities (Figure 4; Table 3), in accordance to expectations [8,10,20,107,116]. Catalyst **1** and **4** give narrow dispersed products. Their distributions can have a polydispersity clearly below two, reminiscent of a Poisson process (Table 3) [90]. The product distribution of these catalysts is generally found in a range below 4. Importantly, the absence of a tail of higher molecular products, typical of Flory-Schulz distributions, which is observed in products prepared by catalysts **2** and **3**.

The reproducibility with respect to the polydispersity index of the distribution of the products prepared with catalysts **1** and **4** is only within this range of 4, the shape is however always similar. The polydispersity index PDIs given correspond to individual experiments, not enough experiments were run for a statistical evaluation. The outcome of the experiments seems to be somewhat dependent on stirring and mixing of the heterogeneous mixture of toluene-swollen reaction mixture. A certain spread of results, e.g., also on account of precipitations of randomly formed higher molecular mass polyethylene with

active catalyst encapsulated and slow exchange of aluminum alkyls with the bulk must be accepted (c.f. Section 3).

Catalysts **2** and **3** give very broad distributions with PDIs over 30 as usual, apparently having a more diverse set of termination and/or propagation reaction rates [20,21,108,111]. Catalyst **5** give very low amounts of low molecular weight products, which were not analyzed by SEC. The main products are soluble 1-olefins [23,78].

Table 3. Characteristics of the products obtained with catalyst **1–4** at various Al (MAO) concentrations.

Compound	[Al] [mmol/L]	Yield [g]	M_n (NMR) [kg/mol]	M_n (SEC abs) [kg/mol]	x_{olefin} [%]	PDI	Shape
1	3	4	9.5	9.0	80	**1.6**	monomodal
	5.5	19.5	7.7	6.7	63	**1.9**	monomodal
	17	24	5.9	5.3	50	**3.5**	monomodal
	22	11	4.9	4.8	40	**1.4**	monomodal
	28	12	4.7	4.6	42	**2.9**	monomodal
	35	13	4.4	3.6	37	**4.2**	monomodal
	45	12	3.2	3.2	30	**1.1**	monomodal
2	3	14	15.7	15.3	27	**32**	broad
	5.5	12	9.0	9.5	13	**38**	broad + shoulder
	20	11	9.7	5.7	15	**130**	broad + shoulder
	28	10.5	4.6	7.8	6	**70**	broad + shoulder
	37	9	8.8	7.2	14	**112**	bimodal
3	3	12	12	10.7	35	**32**	monomodal, broad
	11	11	7.8	10.6	30	**39**	bimodal
	17	8.5	10	7.0	19	**38**	broad + shoulder
	28	9.5	6.7	6.9	29	**72**	bimodal
	35	8	5.4	6.8	11	**78**	bimodal
4	5.5	9	6.2	14.3	32	**1.8**	monomodal
	11	15	4.3	7.0	20	**3.2**	monomodal
	17	11.5	3.1	4.7	25	**3.9**	mm + small shoulder
	22	3	3.1	3.0	<5	**2.3**	mm + small shoulder
	28	5.5	2.8	-	11	-	-
	35	4.5	2.3	-	<5	-	-
	45	6	3.3	-	11	-	-

All experiments were carried out at 10 °C with 0.55–0.8 μmol/L catalyst at 2 bar of ethylene pressure and 40 min (55 min (**1**)) of reaction time.

A simple monomodal distribution is obtained when catalyst **1** is used for the ethylene polymerization (Table 3) [4,107,113]. This system seems to be the most uniform in its catalytic action of the series **1–5**. The molecular weights are well-below 10 kDa under the conditions chosen. This lower range possibly underlies the more simple behavior in terms of distributions and olefin content. The molecular weight decreases globally with the aluminum alkyl concentration, i.e., with the amount of chain starter. The different yields of product in the experiments makes it hard to find direct correlations. This originates from the dissimilar activities of the catalyst-cocatalyst system that are also strongly determined by the amount of MAO in the lower range of concentrations used (Equation (1); Section 3).

The product with the highest olefin content of 80% is found in experiments with catalyst **1** at 3 mmol/L of MAO. Catalyst **1,** in contrast, gives a product mixture with about 30% olefins in combination with cocatalyst MAO at the highest concentration used of 45 mmol/L. The molecular weights of the products obtained under the latter conditions

increase linearly with the ethylene pressure, in accordance to the established rate law (Figure 5b). The olefin content increases also linearly with the ethylene pressure. Several termination processes are obviously simultaneously operative.
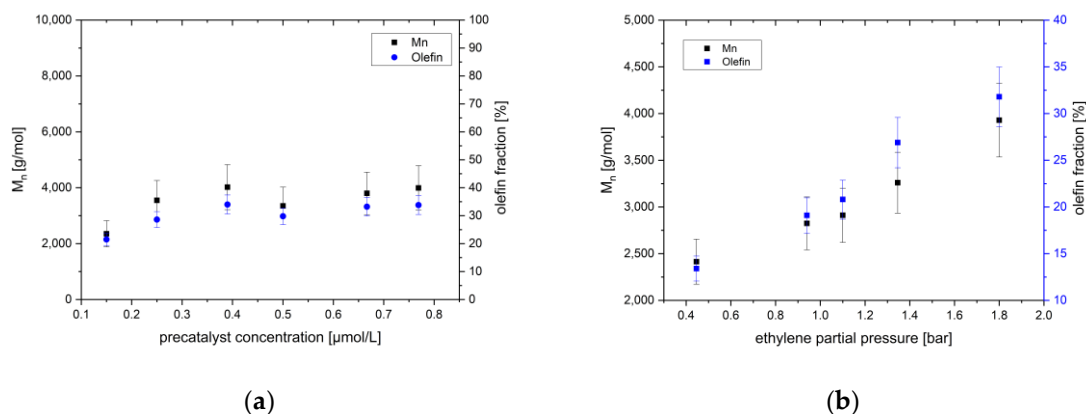

(**a**)   (**b**)

Figure 5. Number average molar mass and olefin content as a function of; (**a**) the catalyst concentration; and (**b**) the monomer pressure. Reaction conditions: 15 °C, 2 bar of ethylene pressure, about 55 min reaction time 45 mmol/L of MAO and for (**b**) 0.6 µmol/L of **1**.

Complex **4** with a methyl and a chloride substituent on the N-aryl of the ligand system has a catalytic action similar to (dichloro) catalyst **1**, involving the relationship between molecular weight and the co-catalyst concentration. The result of the polymerization again is majorly determined by the co-catalyst concentration, which provides anionic chain starters. The inhibition by MAO leads to disappointing low yields at concentrations higher than 20 mmol/L. The shape and the polydispersity of the distribution are similar (somewhat broader) to that of **1**, with the formation of a small amount of a separated second distribution only at higher MAO concentrations. The olefin content under comparable conditions and at comparable yields is much lower than for **1**. The rate of beta-hydrogen elimination seems lower in **4** than in **1**. Somewhat longer chains form at low concentrations of MAO, as fewer chains are formed.

The more electron rich dialkyl catalysts **2** and **3** polymerize ethylene to much broader dispersed product mixtures [20,21,108,111]. Most of the mixtures consist of two overlapping distributions. The molecules at a higher mass particularly contribute to the width of the distribution. The olefin contents tend to be in the same order and below the values obtained with catalyst **4** at similar conditions and yields, indicating an even lower rate of beta-hydrogen elimination. The distributions of the products obtained at low MAO concentrations are dominated by one broad unsymmetrical distribution at much higher mass than of products from **1** and **4**. A higher aluminum content increasingly leads to bimodal molecular weight distributions (MWDs) with the additional distribution appearing (as narrow shoulder) at lower molecular weight.

Catalyst **5** in combination with MAO is also a highly active ethylene oligomerization catalyst for the preparation of α-olefins, but is not suitable for the synthesis of polyethylene with higher molecular weight [23]. Therefore, products with the lowest molecular weights and highest olefin contents were received with the methyl aryl catalyst, where β-hydrogen elimination is the main termination reaction. The proportion of solid products is less than 15 wt% of the ethylene that was consumed during the reaction. Most of these products are liquid olefins with a maximum number of 12 carbon atoms. The solid proportion does not exceed a molecular weight of 1000 g/mol (Figure 6). The concentration of MAO does not have an impact on the molecular weight, and not on the olefin content.
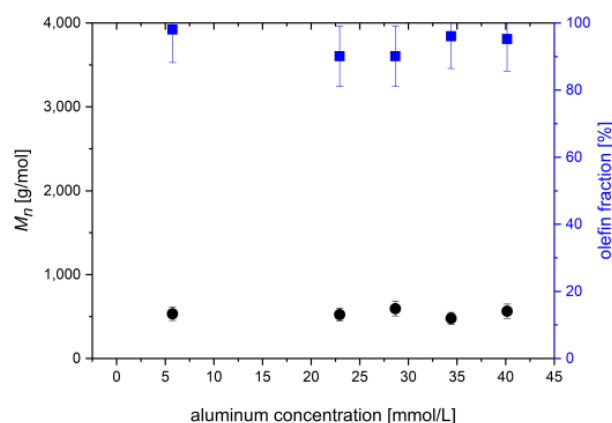
Figure 6. The number average molar mass and olefin fraction of the solid products prepared with catalyst **5**. Reaction conditions: 0.5 µmol/L **5**, 10 °C, 2 bar of ethene pressure, about 40 min reaction time.

3. Discussion

3.1. Propagation Catalysis

The ethylene polymerization, mediated by a set of similar catalyst, was kinetically analyzed with the objective to prepare aluminum polymeryls. Although the target was not immediately reached, a comprehensive mechanism for the simple BIP iron MAO catalyst systems can be deduced. This leads, partly in contrast with other interpretations, to the view of a uniform, single site catalyst system [82,108]. The system comprises a reactive co-catalyst, changing in type and concentration, and a reaction medium with a change of phases (homogenous, heterogeneous with swollen polymer/polymeryls). The line of argumentation will follow the data, obtained in this study, in the same equipment and under similar conditions, and place the current insights into a further perspective.

A common rate law was found, indicating that the catalytic action is based on the same elementary steps. The linear dependence of the rate on the concentration of ethylene and the pre-catalyst points to the rate determining collision between these compounds or its derivatives, and against the existence of a stable iron olefin complex [20,127]. The full amount of pre-catalyst apparently is -as expected- alkylated by MAO to yield the catalytic system. It is conceivable that methylation, and maybe also activation of the pre-catalyst, are achieved by TMA with MAO acting as a soluble carrier [77,97,98,107,128]. Commercial MAO contains, or can form, a variable amount of TMA. There are indications that several aluminum alkyl species coexist in toluene solutions of MAO [7,75–77,80]. These are mobile and thought to be the most relevant in the chain shuttling and for the formation of dormant catalyst. It also explains the observation that not (by far) all of the alkyl entities in MAO initiate a chain.

The (initially) inverse first order dependence of the polymerization rate on the concentration of aluminum alkyls is expected for a pre-equilibrium, which generate the active iron catalyst from a dormant bimetallic iron-aluminum species (Scheme 3) [75]. The derived rate law for a sequence of a pre-equilibrium of a predominantly dormant iron-aluminum alkyl complex (Fe~Al) with a free aluminum alkyl (Al), and the active catalyst (Fe*) with equilibrium constant $K(= [Fe^*][Al]/[Fe \sim Al])$, and a rate determining insertion of free ethylene with rate constant k_p is coincident with Equation (1) (Supplementary Material). The observed rate constant k_{obs} of Equation (1) then equals $k_p K$ (Supplementary Material). The dependence of k_{obs} on the ligand structure, thus, contains contributions related to the equilibrium constant K and the rate of propagation k_p [83,129].

The impact of Lewis acidity on K and k_p may be expected to work in opposite directions with respect to rate of ethylene polymerization. A higher Lewis acidity will lower K, the bimetallic complex of BIP iron alkyls and aluminum alkyls will become more stable. The concentration of the active catalyst decreases. A higher Lewis acidity of the catalyst

center would at the same time yield a more active catalyst with a larger k_p. The necessary polarization by coordination of ethylene to enable nucleophilic attack of an anionic alkyl entity would be reached earlier on the reaction coordinate, and proceed with less activation energy. It must not be surprising that the expected order of increasing Lewis acidity of **3 -> 4 -> 1** is not reflected in the order of polymerization rate **4 -> 1 -> 3** (Table 2). The higher Lewis acidity of **1** is also reflected in the fact that simple aluminum alkyls (TMA, TEA) will not activate the complex for ethylene polymerization. The complexes **1**, **3** and **4** are sterically very alike.

Some reports show that catalysts with electron withdrawing and less bulky aryl substituents have a higher activity [4,20,44,61]. However, the reported experiments were conducted at much lower aluminum concentrations (Al/Fe ratio around 2000). The impact of a low constant *K*, also by a fast change of the co-catalyst identity, then is less strong than at the high MAO concentrations used in this study. The average activity at lower MAO concentrations between 10 and 20 mmol/L show the expected order in activity **3** < **4** ≤ **1** (Table 3). These time average activities should be interpreted with the appropriate reserve, i.e., with knowledge of the time dependence. The influence of sterics on the catalytic action should be considered too in the context of the two factors in comparison of complex **5**, **3** and **2**. A numerical separation of *K* and k_p should be the subject of further studies for understanding the catalytic action, but is experimentally not so easily accessible. The establishment of a general rate law nevertheless gives valuable information on the elementary reaction and coexisting species.
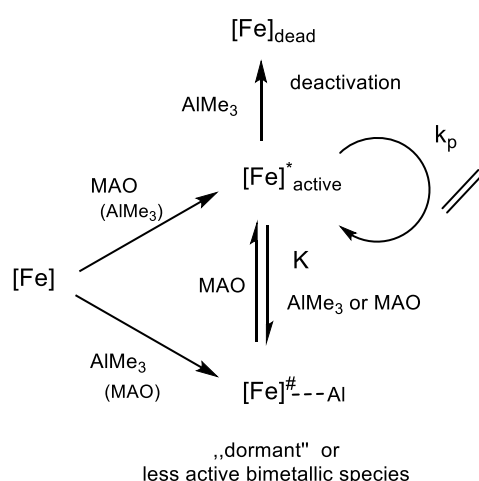
Scheme 3. Ethylene polymerization by bisarylimine iron complexes [Fe] **1**–**5** with MAO containing TMA ([Fe]$^{\#}$ refers to the dormant iron species and [Fe]* to the active form).

The enhancement of the polymerization rate after the first phase can be explained by the transformation of the methyl entities in MAO (and/or the contained TMA) to polymeryl moieties. The coordination ability of larger alkyl groups to BIP iron will be lower, leading to larger values for *K* (more active catalyst). The inhibition of the catalyst by coordination of the aluminum alkyls will be released. Eventually, the aluminum polymeryls reach the solubility limit in the reaction medium on account of their molecular mass. This is at or below 1700 Da in mass (vide infra) [90]. Concomitantly, the observed dependence of the reaction rate on the MAO concentration seems to decline. The more MAO is present, the more ethylene for the transformation into "alkyl aluminoxane" is necessary to observe the effect. Therefore, the time span between the first and second activation process increases with the MAO concentration.

The precipitation of the aluminum (and iron) polymeryls does not necessarily lead to a termination of chain growth as the chain ends may still be accessible in the swollen state [79]. The direct chain shuttling between iron and aluminum polymeryls will have become an unlikely process in the second phase [45,82]. The mixing time may become

a factor as more polymers are formed with the admission of ethylene. The resulting inhomogeneity leads to a distribution of molecular masses and also to the smaller decline of the rate.

3.2. Termination Pathways

The beta-hydrogen elimination and chain shuttling to aluminum are both important termination steps in the catalysts action. A simple correlation between the reaction conditions and olefinic content cannot generally be expected, i.e., next to the spread in the results arising from the heterogeneous character of the system. The number of paraffinic chains is limited by the number of alkyl groups (and potentially by the coordination ability) of the initially provided aluminum methyl groups (in the contained TMA). Note that some smaller paraffins will be lost in the work-up (determined by the volatility and the solubility in the mixture of toluene and ethanol). The number of polyolefins is only determined by the rate of beta-hydrogen elimination and the consecutive new chain growth. The amount increases with ethylene conversion, i.e., with reaction time respectively with activity. This was also observed in former studies, longer reaction times giving more olefinic chains [20,45,130]. The olefin content of aluminum polymeryls could effectively be reduced by decreasing the reaction time and ethylene concentration [91,130].

The bimodal or broad molecular weight distribution of the products received with catalysts **2** and **3** are typical [7,20,54,80,82,131]. The common interpretation is by considering two phases of polymerization. A first stage of irreversible fast chain transfer process leads to the low molecular mass paraffinic products. The second stage is governed by β-H elimination/transfer leading to the higher mass fraction of olefins [45,107]. However, this description remains shy of accounting for the formation of the narrow distributed MWDs of the products of **1** and **4**. In addition, the differences in molecular mass and concentrations of the low molecular mass fraction obtained by the action of catalysts **2** and **3** need a further assessment.

The initial action of catalyst **1** in dependence of the reaction conditions is mostly in agreement with a degenerate living polymerization process involving aluminum-iron alkyl exchange and irreversible beta-hydrogen elimination. The olefin content increases linearly with the ethylene pressure (Figure 5b). The termination along a beta-hydrogen transfer to ethylene is the most simple explanation for this behavior (Scheme 3, bottom process) [20]. This reaction route was also concluded in the study of ethylene oligomerization with BIP iron catalyst bearing one aryl substituent, iron hydrides not being an intermediate [23]. The rate of insertion and of beta-hydrogen transfer are then both linearly dependent on the ethylene concentration, and symmetrically increase with its pressure. It would lead to a Flory-Schulz distribution of polyolefins when this was the only (dominant) process involved. However, this is not the case, the catalyst gives a more narrow distributed mixture of paraffins and olefins of about the same molecular weights (Table 3). The typical shape of a Flory-Schulz distribution with in particular also larger molecular weight components is not found, rather a broadened Poisson-type of distribution results. A reversible exchange of alkyl chains between iron and aluminum centers at a faster (or comparable) time scale than (to) the ethylene insertion can account for this observation. The degenerate exchange with the excess of aluminum alkyls assures that beta-hydrogen transfer on average takes place in an iron complex with an average grown polymeryl entity. The degenerate exchange is also a natural consequence in a system forming dormant species by coordination of aluminum alkyls.

A degenerate chain transfer was reported before in the presence of diethyl zinc but not for aluminum alkyls as chain transfer agents [48,67,90]. The degenerate transfer is operative in a regime, where the zinc alkyls are of lower molecular weight (<2*800 Da). They remain soluble in toluene [90]. The change to a heterogeneous system with precipitated metal alkyls gives a different situation. In contrast, catalyst **1** apparently can still interact with the precipitated aluminum alkyls. Catalyst **1** is also much more active in the chain shuttling as the bisisopropyl aniline based analog, reaching the level of ethylene insertion [90].

The dependence of the molecular weight and the olefin content of the products obtained by the action of catalyst **1** in combination with MAO indicates that basically no olefins are formed in the initial phase. The linear correlation between the olefin content and the M_n leads an offset from the origin of about 1700 Da. About 60 insertions take place before olefins are formed to a substantial extent. Initially, this seems puzzling, as the rate law indicates that aluminum is not coordinated with the active catalyst during olefin insertion, and thus, the rate of a beta-hydrogen transfer cannot be a function of the aluminum concentration. An unchanged ratio between olefin content and molecular weight is expected as both reactions would have a first order dependence on the ethylene concentration.

Steric arguments may be put forward for an understanding. The transition state for beta-hydrogen transfer to ethylene involves a six membered ring with a rather larger demand of space [108]. The interaction of the aryl chloride moieties with aluminum in smaller/soluble aluminum alkyls may temporary enhance the bulk of the axial part of the ligand. Larger aluminum alkyls will start to precipitate at the mass of about 1700 Da and the interaction with the ligand chloride will become of less importance, changing the action of the catalyst [117]. The precipitated aluminums polymeryl are still accessible to the catalyst, the molecular mass uniformly increases (Figure 5b).

Increasing the steric pressure near the catalytic center reduces the probability of a chain termination by the beta-hydrogen transfer and visa versa. This is in particular notable in the action of the sterically most open catalyst **5** (with only one methyl substituent on the aryl part) [23]. The identity of the product mixture is not dependent on the aluminum concentration and very little on the ethylene pressure. Many new chains are initiated and the "Aufbau reaction" with shuttling between aluminum alkyls have little importance. The increased steric extension of the axial ligands of catalyst **3** (Me_2) and **2** (Et_2) on the other hand results in a lower rate of beta-hydrogen transfer, resulting in higher molecular mass products and less olefin formation in the order **5**-**3**-**2**. The products from catalyst **3** and **2** tend to have a Flory-Schulz type of distribution, which is complemented with a further distribution in the low molecular weight region. The latter becomes more important at higher MAO concentrations. The products of this additional distribution obviously results from the transfer reactions with aluminum alkyls, and are all in accordance with reported studies [20,45,107].

These chain shuttling alkyl transfer reactions apparently have a higher rate for catalyst **3** than for **2**. The relative quantity of the low molecular weight distribution is smaller in the polymerization at the sterically most congested active site of catalyst **2**. An explanation involving a direct transfer between formed long chain iron and long chain aluminum alkyls must be challenged (M_n over 5000 Da). The coordination strength of higher alkyl aluminum species is appreciable reduced (rate law in Equation (1)), and most likely the iron and aluminum polymeryls are in a separate phase. The reaction mixture appears turbid soon after the addition of the catalysts, supporting this description.

It was already concluded for catalyst **1** that coordination of the catalyst to the alkyl chain ends of the precipitated aluminum polymeryls is still possible. This can occur when the catalyst is liberated from its growing polymer chain. The remaining termination process to enable this in the swollen precipitated complex is the beta-hydrogen transfer. The formation of longer alkyls on the iron metal is then accompanied by the formation of long chain polyolefins. Formerly aluminum terminated polymers with longer chains are then lost in the process for preparing aluminum polymeryls. Prolonged ethylene polymerization under such a regime will lead to longer chain olefins (as is observed). In case of a more dominant beta-hydrogen transfer as in the second phase of catalyst **1** (with increased beta-hydrogen transfer activity), the grown polymeryls are more and more lost in the form of 1-olefins. The chain growth of the intermediate products is then at the cost of loss of long chain aluminum polymeryls.

Indeed the intensity of the low molecular weight fraction in the products from **3** and **2** goes along with the respective rates of beta-hydrogen transfer. A beta-hydrogen transfer will primary result in the formation of a toluene soluble, mobile cationic iron ethyl derivative (Scheme 4). This compound and its derivatives after the insertion of some ethylene (<~50 units) could react with swollen aluminum alkyls to give a (mobile) aluminum alkyl and an iron coordinated, reactivated chain end. As long as small alkyl groups and accessible chain ends are present, a shuttling of the catalyst along the immobile aluminum polymeryls is then feasible. The concentration of small alkyl groups will determine the amount of active catalysts bound to a swollen precipitated polymeryl entity, and hence, the final mass of the aluminum polymeryls.
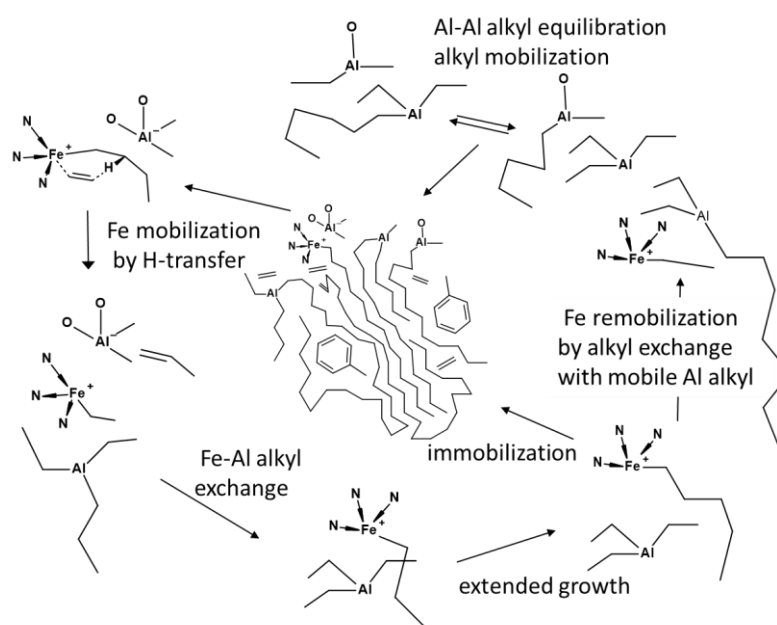
Scheme 4. Reactions in heterophasic BIP iron MAO/TMA catalyzed ethylene polymerization.

The amount of ethylene that is added to the reactor will end up by insertion in the steady state concentrations of the diverse iron alkyls in the reactor. The type of iron alkyls in the catalytic experiments are the time dependent result of all the reactions taken place. The relative rates of alkyl transfer (chain shuttling) with involvement of small alkyls, olefin insertion and beta-hydrogen transfer are most relevant. These will be largely uncoupled in the initial phase i.e., before the precipitation of aluminum polymeryls. The rate of beta-hydrogen transfer relative to insertion becomes important after this phase (in the heterogeneous system that arises), resulting in a coupling of the processes. The product distributions can thus readily be explained under the presumption that small, mobile alkyl group exchange is competitive to the ethylene related reactions. This seems generally to be the case, for catalyst **5** with a dominant beta-hydrogen transfer termination.

The steady state concentration of small aluminum alkyls capable of catalyzing the chain shuttling will be governed by the difference in rates of ethylene insertion, eventually removing the mobile alkyl entity by chain growth, and the beta-hydrogen transfer restoring its presence (Scheme 4). A low rate of beta-hydrogen transfer relative to ethylene insertion will lead to fewer and longer olefinic chains next to smaller aluminum polymeryls (catalyst **2**). A smaller difference (catalyst **3**) will give more and shorter olefinic chains and longer aluminum polymeryls. The concentration of MAO effectively will set the average molecular weight of the polymeryls after completing the ethylene addition (Figure 6).

An even higher relative rate of beta-hydrogen transfer will prevent the formation of a separate olefinic fraction (catalyst **1**, second phase). The yield of aluminum polymeryls will decrease with the mass of the alkyl, and small olefins will increasingly make up the product. These byproducts result from beta-hydrogen transfer in the newly formed alkyls. The

action of catalyst **4** gives evidence for the formation of such a second product distribution at high MAO concentration.

The synthesis of hydroxy-functionalized polyethylene (PEOH) using BIP catalysts was not part of this study, but has been investigated previously [91,102,130]. It has been shown that aluminum polymeryls can be effectively converted into PE-OH [102]. Low to medium molecular weights (1000–6000 g/mol), monomodal distributions and low olefin contents (<20 mol%) are targeted for this purpose. This ensures that the chain ends are accessible for the subsequent oxidation to the aluminum alkoxides. The oxidation with a mixture of dinitrogen dioxygen of 92:8 can be performed in the polymerization reactor after removal of the residual ethylene. The oxidation is not quantitative, and is also more easily achieved for lower molecular weight polymeryls. The formation of products with bimodal MWD is best avoided since the oxidation would preferentially take place on the low molecular weight fraction, and would thus, yield a distribution of products. With the exception of compound **5**, which leads exclusively to short-chain α-olefins, all the investigated catalysts (**1–4**) produce aluminum polymeryls in various proportions and enable the preparation of PE-OH. Catalyst **4** leads to lower olefin fractions, allowing to access higher molecular mass aluminum polymeryls.

4. Materials and Methods

All manipulations of air- and/or moisture-sensitive compounds were carried out under a dry argon atmosphere using standard Schlenk techniques. All aluminum alkyls were used as received and stored at 8 °C. Triethyl aluminum (TEA) was purchased as a 25 wt% solution in toluene from Sigma-Aldrich (Darmstadt, Germany). TMA and TIBA were purchased from Sigma-Aldrich (Darmstadt, Germany) as 2 M solution in toluene. MAO was purchased from Crompton GmbH (Bergkamen, Germany) as 10 wt% solution (ca. 5.25 wt% Al, 1.65 wt% Al as TMA (31 wt% of entire Al), ρ^{20} = 0.884 g/mL, 1.72 mol/L Al) in toluene, aliquots were regularly taken from the 30 L stock. These aliquots were used as intermediate stocks for a maximum of 2 weeks to ensure a constant quality. Nitrogen (purity > 99.996%) was purchased from Praxair Deutschland GmbH (Düsseldorf, Germany) and used as delivered. Toluene was supplied by Merck (Darmstadt, Germany) and purified by distillation and passing through columns filled with molecular sieve (4 Å) and catalyst R3-11/G purchased from BASF (Ludwigshafen am Rhein, Germany). Ethylene was supplied by Westfalen AG (Münster, Germany) and purified by passing through columns filled with molecular sieve (4 Å) and BASF catalyst R3-11/G. Preparation of the pre-catalysts **1–5** was based on reported syntheses [4,20,52,125]. The synthesis is straightforward from the ligand and iron(II) dichloride. The synthesis of the ligands is from diacetyl pyridine and the corresponding aniline derivate. The starting materials and solvents were supplied from Sigma Aldrich (Darmstadt, Germany), Alfa Aesar (Heysham, Lanashire, UK), Acros Organics (Fair Lawn, NJ, USA), abcr (Karlsruhe, Germany) and VWR International GmbH (Darmstadt, Germany). The pre-catalysts were suspended in dry toluene and stored at 8 °C.

The catalysts are used as suspension in toluene in very small concentrations. The catalyst suspensions were stirred while the desired amount of catalyst for the respective experiment was measured with a syringe. Injection of the catalyst suspension can be subject of experimental errors since catalyst particles can stick on the reactor wall or remain in the syringe after injection.

The determination of the constants k' are based on a multiple determinations. The other reported results are mostly based on single experiments for a single condition. A general reproducibility can still be confirmed from a random sample survey and the results of former studies that are not reported in this paper. A spread of results is obtained, the system reacts very in a sensitive manner to little variations in the set up and course.

4.1. Standard Procedure for Semi Batch and Batch Polymerizations

All polymerizations were carried out in 1 L stainless steel reactors equipped with an anchor mixer (BEP 280 Büchiglas (Büchi AG, Uster, Swizerland)) that were previously heated at 600 °C with a hot air gun and dried under a dynamic vacuum for at least one hour. The reactor was cooled to the desired reaction temperature and filled with 300 mL of toluene, followed by nitrogen up to 50 mbar above local atmospheric pressure. The target amount of cocatalyst-solution was added, using standard Schlenk techniques. The solution was saturated with ethylene to the intended pressure. The reaction was started by injecting the desired amount of the BIP iron(II) dichloride pre-catalyst as suspension in toluene into the reactor. The consumed ethylene was calculated from the formal uptake of the volume and normalized to 1 bar, i.e., the measured volume was divided by the time dependent pressure of uptake. The reaction was quenched upon reaching atmospheric pressure or steady vessel pressure. In semi-batch reactions, the excess ethylene was discharged, and the reaction was quenched after a certain reaction time. Quenching was performed by adding small aliquots (5–20 mL) of ethanol. To complete the quenching, the reaction mixture was stirred for an additional hour with 200 mL of a quenching solution (2M hydrochloric acid in water and ethanol) The precipitated product was filtered, washed with ethanol and dried in vacuo at 40 °C before characterization.

4.2. Characterization

NMR Data was obtained using a AVANCEIII HD 600 MHz spectrometer from Bruker (Billerica, MA, USA). 20–25 mg polymer was dissolved in 0.65 mL 1,2,4-trichlorbenzene with 0.05 mL 1,1,2,2-tetrachlorethane-d_2 as locking standard and measured at 100 °C to ensure a high degree of solvation. Molecular weight distributions were determined via high temperature size exclusion chromatography using a PL-GPC-220 from Agilent (Santa Clara, CA, USA) with a refractive index detector and 1,2,4-trichlorbenzene as solvent. Measurements were performed at 135 °C and evaluated using a polystyrene calibration. The results of SEC experiments have been corrected using the Kuhn-Mark-Houwink-Sakurada equation to give (close to) absolute values [132].

5. Conclusions

The reaction kinetics of the chain propagation of ethylene polymerization with five different bisimine pyridine iron dichlorides catalysts cocatalyzed by methyl aluminoxane was mapped. The chain propagation exhibited a clean, not so often observed first-order kinetics with respect to both monomer and catalyst concentration; aluminum alkyls inhibit the formation of the active catalyst from the corresponding iron alkyls. The inhibition by aluminum alkyls is a function of the molecular weights of the alkyls. It is released by increasing the length of the alkyls on account of the coordination ability and the incompatibility to the toluene reaction medium. Both electronic and steric properties of the phenyl substituents of the aryl imine entity influence the catalytic action. The reaction steps in the catalysis involve a dissociation of aluminum alkyls from (cationic) iron alkyls, ethylene insertion, alkyl exchange and beta-hydrogen transfer reactions.

Electron-withdrawing substituents in the ligand yield more Lewis acidic centers. The concentration of the active catalyst is lower with such centers, and all the processes are generally faster. This leads to a degenerate ethylene polymerization in catalysts **1** and **4**, with option of providing narrow distributed products. The beta-hydrogen transfer in catalyst **1** is much faster than in **4**, and with conversion of ethylene, and thus, with molecular mass, the product mixture becomes predominantly olefinic. Only low molecular mass aluminum alkyls are accessible with catalyst **1**.

Bulkier ligands are unfavorable for reaching the transition state of beta-hydrogen transfer. This results in the formation of long alkyl chains as soon as the chain shuttling becomes slow. The lower rate of alkyl exchange between aluminum and iron under such conditions results from the lower stability of heterobimetallic complexes of aluminum and iron alkyls, and in a later stage, predominantly by the low mobility of the swollen/precipitated alu-

minum polymeryls. The rate of beta-hydrogen transfer then is the product determining reaction as it is the alternative entrance to chain shuttling. Overall, catalyst **4** seems to show the best performance for obtaining aluminum polymeryls. The moderate rate of beta-hydrogen transfer gives intermediate mobile iron alkyls, capable of reactivating the precipitated aluminum polymeryls. The rate of ethylene insertion is in the order of chain shuttling, leading to a degenerate chain growth.

Based on the results, it can be concluded that a BIP catalyst with electron withdrawing and moderately bulky substituents at the phenyl rings lead to products that are most suitable for the synthesis of PEOH. It is a matter of finding a balance between inactivation through the formation of bi-metallics, and competition between insertion, beta-hydrogen transfer and chain shuttling. Alpha chlorinated methyl substituents on the ligand of catalyst **2** could lead to a promising polymerization catalyst for the one pot synthesis of functionalized polyethylene.

Supplementary Materials: The following are available online at https://www.mdpi.com/2073-4344/11/3/407/s1, Figure S1: Plot of ethylene dissolved in 300 mL of toluene with 45 mmol/L MAO at various ethylene partial pressures at 15 °C, Figure S2: Time dependent ethene volume flow during the polymerization mediated by catalyst **1** (45 mmol/L Al (MAO), 0.33 μmol/L of **1**, 15 °C, 2 bar of ethene pressure), Figure S3: Ethylene massflow (normalized to 1 bar ethene) at varying aluminum concentrations during polymerization catalysis by **4**. Reaction conditions: 0.8 μmol/L catalyst, 10 °C, 2 bars of ethylene, Figure S4: Ethylene massflow (normalized to 1 bar ethene) at varying aluminum concentrations during polymerization catalysis by **2**. The inconsistencies at 2.8 mmol/L Al result from a temporarily technical problem with the massflow controller. Reaction conditions: 0.6 μmol/L catalyst, 10 °C, 2 bars of ethylene, Figure S5: Ethylene massflow at varying aluminum concentrations during polymerization catalysis by **1**. Reaction conditions: 0.6 μmol/L catalyst, 15 °C, 2 bars of ethylene, Figure S6: Ethylene massflow (normalized to 1 bar ethene) at varying aluminum concentrations during polymerization catalysis by **5**. Reaction conditions: 0.5 μmol/L catalyst, 10 °C, 2 bars of ethylene, Figure S7: Normalized logarithmic ethylene pressure loss against the reaction time for catalyst **2**. Reaction conditions: 0.5 μmol/L catalyst, 40 mmol/L of MAO, 5 °C, 1–3 bar ethylene, Figure S8. Normalized logarithmic ethylene pressure loss against the reaction time for catalyst **3**. Reaction conditions: 0.5 μmol/L catalyst, 40 mmol/L of MAO, 5 °C, 1–3 bar ethylene, Figure S9: Normalized logarithmic ethylene pressure loss against the reaction time for catalyst **5**. Reaction conditions: 0.3 μmol/Lcatalyst, 40 mmol/L of MAO, 5 °C, 1–3 bar ethylene, Figure S10: Normalized logarithmic ethylene pressure loss against the reaction time for catalyst **4**. Reaction conditions: 0.8 μmol/L catalyst, 40 mmol/L of MAO, 5 °C, 1–3 bar ethylene, Table S1: Slopes of the regression lines of the respective kinetic studies with confidence interval. For reaction conditions see description of respective Figure (Figures 4–6, Figures S7–S10).

Author Contributions: Conceptualization, G.A.L. and E.M.S.; investigation, E.M.S.; formal analysis, E.M.S. and G.A.L.; writing—original draft preparation, E.M.S.; writing—review and editing, G.A.L. and E.M.S.; visualization, E.M.S. and G.A.L.; supervision, G.A.L. All authors have read and agreed to the published version of the manuscript.

Conflicts of Interest: The authors declare no conflict of interest.

References

1. Plastics –the Facts 2020. Available online: http://www.plasticeurope.org (accessed on February 2020).
2. Schilling, M.; Bal, R.; Go, C.; Alt, H.G. Heterogeneous Catalyst Mixtures for the Polymerization of Ethylene. *Polymer* **2007**, *48*, 7461–7475. [CrossRef]
3. Stürzel, M.; Mihan, S.; Mülhaupt, R. Multisite Polymerization Catalysis to Sustainable Materials and All-Polyolefin Composites. *Chem. Rev.* **2016**, *116*, 1398–1433. [CrossRef]
4. Chen, Y.; Chen, R.; Qian, C.; Dong, X.J.; Sun, W.H. Halogen-substituted 2, 6-Bis (imino) Pyridyl Iron and Cobalt Complexes: Highly Active Catalysts for Polymerization and Oligomerization of Ethylene. *Organometallics* **2003**, *22*, 4312–4321. [CrossRef]

5. Kindler, H.; Nikles, A. Energieaufwand zur Herstellung von Werkstoffen-Berechnungsgrundsätze und Energieäquivalenzwerte von Kunststoffen. *Kunststoff* **1980**, *70*, 802–807.

6. Mecking, S. Olefin Polymerisation durch Komplexe später Übergangsmetalle–ein Wegbereiter der Ziegler Katalysatoren erscheint in neuem Gewand. *Angew. Chem.* **2001**, *113*, 550–557. [CrossRef]

7. Semikolenova, N.V.; Zakharov, V.A.; Echevskaja, L.G.; Matsko, M.A.; Bryliakov, K.P.; Talsi, E.P. Homogeneous Catalysts for Ethylene Polymerization Based on Bis(Imino)Pyridine Complexes of Iron, Cobalt, Vanadium and Chromium. *Catal. Today* **2009**, *144*, 334–340. [CrossRef]

8. Flisak, Z.; Sun, W.H. Progression of Diiminopyridines: From Single Application to Catalytic Versatility. *ACS Catal.* **2015**, *5*, 4713–4724. [CrossRef]

9. Boudier, A.; Breuil, P.A.R.; Magna, L.; Olivier-Bourbigou, H.; Braunstein, P. Ethylene Oligomerization using Iron Complexes: Beyond the Discovery of Bis(imino)pyridine Ligands. *Chem. Commun.* **2014**, *50*, 1398–1407. [CrossRef]

10. Small, B.L. Discovery and Development of Pyridine-Bis(imine) and Related Catalysts for Olefin Polymerization and Oligomerization. *Acc. Chem. Res.* **2015**, *48*, 2599–2611. [CrossRef] [PubMed]

11. Burcher, B.; Breuil, P.A.R.; Magna, L.; Olivier-Bourbigou, H. Iron-Catalyzed Oligomerization and Polymerization Reactions. In *Iron Catalysis II. Topics in Organometallic Chemistry*; Bauer, E., Ed.; Springer: Cham, Switzerland, 2015; Volume 50, pp. 217–257.

12. Sun, W.H. Novel Polyethylenes via Late Transition Metal Complex Pre-Catalysts. In *Polyolefins: 50 Years after Ziegler and Natta II. Advances in Polymer Science*; Kaminsky, W., Ed.; Springer: Berlin/Heidelberg, Germany, 2013; Volume 258, pp. 163–178.

13. Takeuchi, D. Olefin Polymerization with Non-Metallocene Catalysts (Late Transition Metals). In *Organometallic Reactions and Polymerization. Lecture Notes in Chemistry*; Osakada, K., Ed.; Springer: Berlin/Heidelberg, Germany, 2014; Volume 85, pp. 119–167.

14. Vaidya, T.; Klimovica, K.; LaPointe, A.M.; Keresztes, I.; Lobkovsky, E.B.; Daugulis, O.; Coates, G.W. Secondary Alkene Insertion and Precision Chain-Walking: A New Route to Semicrystalline "Polyethylene" from α-Olefins by Combining Two Rare Catalytic Events. *J. Am. Chem. Soc.* **2014**, *136*, 7213–7216. [CrossRef]

15. Long, B.K.; Eagan, J.M.; Mulzer, M.; Coates, G.W. Semi-Crystalline Polar Polyethylene: Ester-Functionalized Linear Polyolefins Enabled by a Functional Group Tolerant Cationic Nickel Catalyst. *Angew. Chem. Int. Ed.* **2016**, *55*, 7106–7110. [CrossRef]

16. Tran, Q.H.; Brookhart, M.; Daugulis, O. New Neutral Nickel and Palladium Sandwich Catalysts: Synthesis of Ultra-High Molecular Weight Polyethylene (UHMWPE) via Highly Controlled Polymerization and Mechanistic Studies of Chain Propagation. *J. Am. Chem. Soc.* **2020**, *142*, 7198–7206. [CrossRef]

17. Chen, Z.; Leatherman, M.D.; Daugulis, O.; Brookhart, M. Nickel-Catalyzed Copolymerization of Ethylene and Vinyltrialkoxysilanes: Catalytic Production of Cross-linkable Polyethylene and Elucidation of the Chain-Growth Mechanism. *J. Am. Chem. Soc.* **2017**, *139*, 16013–16022. [CrossRef]

18. Rhinehart, J.L.; Brown, L.A.; Long, B.K. A Robust Ni (II) α-Diimine Catalyst for High Temperature Ethylene Polymerization. *J. Am. Chem. Soc.* **2013**, *135*, 16316–16319. [CrossRef] [PubMed]

19. Carrow, B.P.; Nozaki, K. Transition-metal-catalyzed Functional Polyolefin Synthesis: Effecting Control through Chelating Ancillary Ligand Design and Mechanistic Insights. *Macromolecules* **2014**, *47*, 2541–2555. [CrossRef]

20. Britovsek, G.J.P.; Bruce, M.; Gibson, V.C. Iron and Cobalt Ethylene Polymerization Catalysts bearing 2, 6-Bis (imino) Pyridyl Ligands: Synthesis, Structures, and Polymerization Studies. *J. Am. Chem. Soc.* **1999**, *121*, 8728–8740. [CrossRef]

21. Britovsek, G.J.P.; Gibson, V.C.; McTavish, S.J.; Solan, G.A.; White, A.J.P.; Williams, D.J.; Kimberly, B.S.; Maddox, P.J. Novel Olefin Polymerization Catalysts Based on Iron and Cobalt. *Chem. Commun.* **1998**, *311*, 849–850. [CrossRef]

22. Small, B.L.; Brookhart, M.; Bennett, A.M. Highly Active Iron and Cobalt Catalysts for the Polymerization of Ethylene. *J. Am. Chem. Soc.* **1998**, *7863*, 4049–4050. [CrossRef]

23. Small, B.L.; Brookhart, M. Iron-based Catalysts with Exceptionally High Activities and Selectivities for Oligomerization of Ethylene to Linear α-Olefins. *J. Am. Chem. Soc.* **1998**, *120*, 7143–7144. [CrossRef]

24. Britovsek, G.J.P.; Gibson, V.C.; Wass, D.F. Auf der Suche nach einer neuen Generation von Katalysatoren zur Olefinpolymerisation: "Leben" jenseits der Metallocene. *Angew. Chem.* **1999**, *111*, 448–468. [CrossRef]

25. Ittel, S.D.; Johnson, L.K.; Brookhart, M. Late-metal Catalysts for Ethylene Homo-and Copolymerization. *Chem. Rev.* **2000**, *100*, 1169–1203. [CrossRef] [PubMed]

26. Bianchini, C.; Giambastiani, G.; Guerrero Rios, I.; Mantovani, G.; Meli, A.; Segarra, A.M. Ethylene Oligomerization, Homopolymerization and Copolymerization by Iron and Cobalt Catalysts with 2, 6-(Bis-organylimino) Pyridyl Ligands. *Coord. Chem. Rev.* **2006**, *250*, 1391–1418. [CrossRef]

27. Gibson, V.C.; Solan, G.A. Olefin Oligomerizations and Polymerizations Catalyzed by Iron and Cobalt Complexes Bearing Bis(imino)pyridine Ligands. In *Catalysis without Precious Metals*; Bullock, M., Ed.; Wiley-VCH: Weinheim, Germany, 2010; pp. 111–141.

28. Gibson, V.C.; Solan, G.A. Iron-Based and Cobalt-Based Olefin Polymerisation Catalysts. In *Metal Catalysts in Olefin Polymerization*; Guan, Z., Ed.; Springer: Berlin/Heidelberg, Germany, 2009; Volume 26, pp. 107–158.

29. Zhang, W.; Sun, W.H.; Redshaw, C. Tailoring Iron Complexes for Ethylene Oligomerization and/or Polymerization. *Dalton Trans.* **2013**, *42*, 8988–8997. [CrossRef] [PubMed]

30. Bianchini, C.; Giambastiani, G.; Luconi, L.; Meli, A. Olefin Oligomerization, Homopolymerization and Copolymerization by Late Transition Metals Supported by (Imino) Pyridine Ligands. *Coord. Chem. Rev.* **2010**, *254*, 431–455. [CrossRef]

31. Ma, J.; Feng, C.; Wang, S.; Zhao, K.Q.; Sun, W.H.; Redshaw, C.; Solan, G.A. Bi-and Tri-dentate Imino-Based Iron and Cobalt Pre-Catalysts for Ethylene Oligo-/Polymerization. *Inorg. Chem. Front.* **2014**, *1*, 14–34. [CrossRef]

32. Britovsek, G.J.; Mastroianni, S.; Solan, G.A.; Baugh, S.P.; Redshaw, C.; Gibson, V.C.; Elsegood, M.R. Oligomerisation of Ethylene by Bis (imino)pyridyliron and Cobalt Complexes. *Chem. A Eur. J.* **2000**, *6*, 2221–2231. [CrossRef]

33. Baier, M.C.; Zuideveld, M.A.; Mecking, S. Post-Metallocenes. *Angew. Chem. Int. Ed.* **2014**, *53*, 9722–9744. [CrossRef]

34. Domski, G.J.; Rose, J.M.; Coates, G.W.; Bolig, A.D.; Brookhart, M. Living Alkene Polymerization: New Methods for the Precision Synthesis of Polyolefins. *Prog. Polym. Sci.* **2007**, *32*, 30–92. [CrossRef]

35. Gibson, V.C.; Redshaw, C.; Solan, G.A. Bis (imino) Pyridines: Surprisingly Reactive Ligands and a Gateway to new Families of Catalysts. *Chem. Rev.* **2007**, *107*, 1745–1776. [CrossRef]

36. Zhang, W.; Guo, J.; Sun, W.H.; Guo, L.; Zhu, D. Preparation of Iron Complex Catalyst for Polymerization of Ethylene. CN111848843A, 30 October 2020.

37. Lin, W.; Zhang, L.; Gao, J.; Zhang, Q.; Ma, Y.; Liu, H.; Sun, W.H. 6-Arylimino 2-(2-(1-phenylethyl) naphthalen-1-yl)-iminopyridylmetal (Fe and Co) Complexes as Highly Active Precatalysts for Ethylene Polymerization: Influence of Metal and/or Substituents on the Active, Thermostable Performance of Their Complexes and Resultant Polyethylenes. *Molecules* **2020**, *25*, 4244.

38. Zhang, W.; Guo, J.; Sun, W.H.; Guo, L.; Zhu, D. Imine Metal Complex Catalyst, Preparing Method Thereof and Application Thereof in Ethylene Polymerization. CN111718382A, 29 September 2020.

39. Zhang, Q.; Zhang, R.; Han, M.; Yang, W.; Liang, T.; Sun, W.H. 4,4′-Difluorobenzhydryl-modified Bis (imino)-pyridyliron (II) Chlorides as Thermally Stable Precatalysts for Strictly Linear Polyethylenes with Narrow Dispersities. *Dalton Trans.* **2020**, *49*, 7384–7396. [CrossRef] [PubMed]

40. Khoshsefat, M.; Dechal, A.; Ahmadjo, S.; Mortazavi, S.M.M.; Zohuri, G.; Soares, J.B. Amorphous to High Crystalline PE Made by Mono and Dinuclear Fe-based Catalysts. *Eur. Polym. J.* **2020**, *119*, 229–238. [CrossRef]

41. Yang, W.; Ma, Z.; Yi, J.; Ahmed, S.; Sun, W.H. Catalytic Performance of Bis(imino) Pyridine Fe/Co Complexes Toward Ethylene Polymerization by 2D-/3D-QSPR Modeling. *J. Comput. Chem.* **2019**, *40*, 1374–1386. [CrossRef] [PubMed]

42. Ahmed, S.; Yang, W.; Ma, Z.; Sun, W.H. Catalytic Activities of Bis (pentamethylene) Pyridyl (Fe/Co) Complex Analogues in Ethylene Polymerization by Modeling Method. *J. Phys. Chem. A* **2018**, *122*, 9637–9644. [CrossRef] [PubMed]

43. Cordeiro, S.; Pereira, L.; Simoes, M.D.O.; Marques, M.D.F. Synthesis and Evaluation of New Bis{imino) Pyridine Based Catalysts for Ethylene Polymerization. *Chem. Chem. Tech.* **2016**, *10*, 413–421. [CrossRef]

44. Wang, Z.; Solan, G.A.; Ma, Y.; Liu, Q.; Liang, T.; Sun, W.H. Fusing Carbocycles of Inequivalent Ring Size to a Bis (imino) pyridine-Iron Ethylene Polymerization Catalyst: Distinctive Effects on Activity, PE Molecular Weight and Dispersity. *Research* **2019**, *2019*, 1–15. [CrossRef] [PubMed]

45. Reinhart, E.D.; Jordan, R.F. Synthesis and Ethylene Reactivity of Dinuclear Iron and Cobalt Complexes Supported by Macrocyclic Bis(pyridine-diimine) Ligands Containing o-Terphenyl Linkers. *Organometallics* **2020**, *39*, 2392–2404. [CrossRef]

46. Han, M.; Zhang, Q.; Oleynik, I.I.; Suo, H.; Oleynik, I.V.; Solan, G.A.; Sun, W.H. Adjusting Ortho-Cycloalkyl Ring Size in a Cycloheptyl-Fused N, N, N-Iron Catalyst as Means to Control Catalytic Activity and Polyethylene Properties. *Catalysts* **2020**, *10*, 1002. [CrossRef]

47. Li, G.; Ge, Y.; Xu, G.; Dai, S. The Electronic Effects on Unsymmetrical Bis (imino) Pyridyl Iron (II) Catalyzed Ethylene Polymerization. *J. Organomet. Chem.* **2020**, *923*, 121457. [CrossRef]

48. Khoshsefat, M.; Dechal, A.; Ahmadjo, S.; Mortazavi, M.M.; Zohuri, G.H.; Soares, J.B. Zn-assisted Cooperative Effect for Copolymers made by Heterodinuclear Fe− Ni Catalyst. *ChemCatChem* **2020**, *12*, 5809–5818. [CrossRef]

49. Zada, M.; Vignesh, A.; Suo, H.; Ma, Y.; Liu, H.; Sun, W.H. NNN-type Iron (II) Complexes Consisting Sterically Hindered Dibenzocycloheptyl Group: Synthesis and Catalytic Activity towards Ethylene Polymerization. *Mol. Catal.* **2020**, *492*, 110981. [CrossRef]

50. Semikolenova, N.V.; Panchenko, V.N.; Paukshtis, E.A.; Matsko, M.A.; Zakharov, V.A. Study of Supported Catalysts, Prepared via Binding of Fe (II) Bis (imino) Pyridyl Complex with Silica, Modified by Alumina: Effect of Surface Lewis Acidic Sites on Catalyst Composition and Activity in Ethylene Polymerization. *Mol. Catal.* **2020**, *486*, 110878. [CrossRef]

51. Zhang, R.; Han, M.; Ma, Y.; Solan, G.A.; Liang, T.; Sun, W.H. Steric and Electronic Modulation of Iron Catalysts as a Route to Remarkably High Molecular Weight Linear Polyethylenes. *Dalton Trans.* **2019**, *48*, 17488–17498. [CrossRef]

52. Britovsek, G.J.P.; Clentsmitha, G.K.B.; Gibson, V.C.; Goodgame, D.M.L.; McTavish, S.J.; Pankhurst, Q.A. The Nature of the Active Site in Bis(imino)pyridine Iron Ethylene Polymerisation Catalysts. *Catal. Commun.* **2002**, *3*, 207–211. [CrossRef]

53. Guo, L.; Liu, Y.; Lian, K.; Sun, W.; Zhu, H.; Du, Q.; Dai, S. Electronic Effects of the Backbone on Bis (imino) pyridyliron (II)-Catalyzed Ethylene Polymerization. *Eur. J. Inorg. Chem.* **2018**, *45*, 4887–4892. [CrossRef]

54. Bryliakov, K.P.; Semikolenova, N.V.; Zudin, V.N.; Zakharov, V.A.; Talsi, E.P. Ferrous Rather than Ferric Species are the Active Sites in Bis (imino) Pyridine Iron Ethylene Polymerization Catalysts. *Catal. Commun.* **2004**, *5*, 45–48. [CrossRef]

55. Chen, Y.; Qian, C.; Sun, J. Fluoro-substituted 2,6-Bis (imino) Pyridyl Iron and Cobalt Complexes: High-activity Ethylene Oligomerization Catalysts. *Organometallics* **2003**, *22*, 1231–1236. [CrossRef]

56. Kawakami, T.; Ito, S.; Nozaki, K. Iron-catalysed Homo-and Copolymerisation of Propylene: Steric Influence of Bis (Imino) Pyridine Ligands. *Dalton Trans.* **2015**, *44*, 20745–20752. [CrossRef] [PubMed]

57. Wang, Z.; Solan, G.A.; Zhang, W.; Sun, W.-H. Carbocyclic Fused N, N, N-Pincer Ligands as Ring-Strain Adjustable Supports for Iron and Cobalt Catalysts in Ethylene Oligo-/Polymerization. *Coord. Chem. Rev.* **2018**, *363*, 92–108. [CrossRef]

58. Zhang, Y.; Wang, C.; Jian, Z. A Comprehensive Study on Highly Active Pentiptycenyl-substituted Bis (Imino) Pyridyl Iron (II) Mediated Ethylene Polymerization. *Eur. Polym. J.* **2020**, *128*, 109605. [CrossRef]

59. Guo, L.H.; Gao, H.Y.; Zhang, L.; Zhu, F.M.; Wu, Q. An Unsymmetrical Iron (II) Bis (Imino) Pyridyl Catalyst for Ethylene Polymerization: Effect of a Bulky Ortho Substituent on the Thermostability and Molecular Weight of Polyethylene. *Organometallics* **2010**, *29*, 2118–2125. [CrossRef]

60. Bariashir, C.; Wang, Z.; Ma, Y.; Vignesh, A.; Hao, X.; Sun, W.H. Finely Tuned α, α′-Bis (arylimino)-2, 3: 5, 6-bis (pentamethylene) Pyridine-Based Practical Iron Precatalysts for Targeting Highly Linear and Narrow Dispersive Polyethylene Waxes with Vinyl ends. *Organometallics* **2019**, *38*, 4455–4470. [CrossRef]

61. Mahmood, Q.; Yue, E.; Guo, J.; Zhang, W.; Ma, Y.; Hao, X.; Sun, W.H. Nitro-functionalized Bis (imino) Pyridyl Ferrous Chlorides as Thermo-stable Precatalysts for Linear Polyethylenes with High Molecular Weights. *Polymer* **2018**, *159*, 124–137. [CrossRef]

62. Wang, Z.; Zhang, R.; Zhang, W.; Solan, G.A.; Liu, Q.; Liang, T.; Sun, W.H. Enhancing Thermostability of Iron Ethylene Polymerization Catalysts through N, N, N-chelation of Doubly Fused α, α′-Bis(arylimino)-2,3:5,6-bis(hexamethylene) Pyridines. *Catal. Sci. Technol.* **2019**, *9*, 1933–1943. [CrossRef]

63. Zhang, W.; Chai, W.; Sun, W.H.; Hu, X.; Redshaw, C.; Hao, X. 2-(1-(Arylimino) Ethyl)-8-arylimino-5, 6, 7-trihydroquinoline Iron (II) Chloride Complexes: Synthesis, Characterization, and Ethylene Polymerization Behavior. *Organometallics* **2012**, *31*, 5039–5048. [CrossRef]

64. Zhao, W.; Yue, E.; Wang, X.; Yang, W.; Chen, Y.; Hao, X.; Sun, W.H. Activity and Stability Spontaneously Enhanced Toward Ethylene Polymerization by Employing 2-(1-(2, 4-dibenzhydrylnaphthylimino) Ethyl)-6-(1-(arylimino) Ethyl) Pyridyl Iron (II) Dichlorides. *J. Polym. Sci. Part A Polym. Chem.* **2017**, *55*, 988–996. [CrossRef]

65. Guo, J.; Zhang, W.; Oleynik, I.I.; Solan, G.A.; Oleynik, I.V.; Liang, T.; Sun, W.H. Probing the Effect of Ortho-cycloalkyl Ring Size on Activity and Thermostability in Cycloheptyl-fused N,N,N-iron Ethylene Polymerization Catalysts. *Dalton Trans.* **2020**, *49*, 136–146. [CrossRef] [PubMed]

66. Suo, H.; Li, Z.; Oleynik, I.V.; Wang, Z.; Oleynik, I.I.; Ma, Y.; Sun, W.H. Achieving Strictly Linear Polyethylenes by the NNN-Fe Precatalysts Finely Tuned with Different Sizes of Ortho-cycloalkyl Substituents. *Appl. Organomet. Chem.* **2020**, *34*, 25937. [CrossRef]

67. Pereira, L.Q.; Cordeiro, S.B.; Cosme, M.S.; Marques, M.F. Influence of Diethylzinc on Ethylene Polymerization Using Iron Catalyst Homogeneous and Supported on Clay. *Appl. Catal. A Gen.* **2014**, *475*, 179–185. [CrossRef]

68. Cordeiro, S.B.; Maria de Fatima, V.M. Evaluation of Bis(imino)pyridine Iron Catalyst on Heterogeneous Ethylene Polymerization. *Chem. Chem. Technol.* **2020**, *14*, 185–194. [CrossRef]

69. Chen, M.; Chen, Y.; Li, W.; Dong, C.; Liang, P.; Wang, N.; Yang, Y. Selective Distribution and Contribution of Nickel Based Pre-catalyst in the Multisite Catalyst for the Synthesis of Desirable Bimodal Polyethylene. *Eur. Polym. J.* **2020**, *135*, 109878. [CrossRef]

70. Takeuchi, D. Oligomerization of Olefins. In *Organometallic Reactions and Polymerization*; Osakada, K., Ed.; Springer: Berlin/Heidelberg, Germany, 2014; Volume 85, pp. 169–215.

71. Champouret, Y.; Hashmi, O.H.; Visseaux, M. Discrete Iron-based Complexes: Applications in Homogeneous Coordination-Insertion Polymerization Catalysis. *Coord. Chem. Rev.* **2019**, *390*, 127–170. [CrossRef]

72. Delle Chiaie, K.R.; Biernesser, A.B.; Ortuño, M.A.; Dereli, B.; Iovan, D.A.; Wilding, M.J.T.; Byers, J.A. The Role of Ligand Redox Non-innocence in Ring-opening Polymerization Reactions Catalysed by Bis(imino) Pyridine Iron Alkoxide Complexes. *Dalton Trans.* **2017**, *46*, 12971–12980. [CrossRef] [PubMed]

73. Babik, S.T.; Fink, G. Propylene Polymerization with a Bisiminepyridine Iron Complex: Activation with Ph₃C[B (C₆F₅)₄] and AlR₃; Iron Hydride Species in the Catalytic Cycle. *J. Mol. Catal. A Chem.* **2002**, *188*, 245–253. [CrossRef]

74. Chen, E.Y.; Marks, T.J. Cocatalysts for Metal-catalyzed Olefin Polymerization: Activators, Activation Processes and Structure−Activity Relationships. *Chem. Rev.* **2000**, *100*, 1391–1434. [CrossRef] [PubMed]

75. Wang, S.; Liu, D.; Huang, R.; Zhang, Y.; Mao, B. Studies on the Activation and Polymerization Mechanism of Ethylene Polymerization Catalyzed by Bis (imino) Pyridyl Iron (II) Precatalyst with Alkylaluminum. *J. Mol. Catal. A Chem.* **2006**, *245*, 122–131. [CrossRef]

76. Soshnikov, I.E.; Semikolenova, N.V.; Bushmelev, A.N.; Bryliakov, K.P.; Lyakin, O.Y.; Redshaw, C.; Zakharov†, V.A.; Talsi, E.P. Investigating the Nature of the Active Species in Bis (imino) Pyridine Cobalt Ethylene Polymerization Catalysts. *Organometallics* **2009**, *28*, 6003–6013. [CrossRef]

77. Bryliakov, K.P.; Semikolenova, N.V.; Zakharov, V.A.; Talsi, E.P. Active Intermediates of Ethylene Polymerization over 2, 6-Bis (imino) Pyridyl Iron Complex Activated with Aluminum Trialkyls and Methylaluminoxane. *Organometallics* **2004**, *4*, 5375–5378. [CrossRef]

78. Hanton, M.J.; Tenza, K. Bis(Imino)Pyridine Complexes of the First-Row Transition Metals: Alternative Methods of Activation. *Organometallics* **2008**, *27*, 5712–5716. [CrossRef]

79. Wang, Q.; Yang, H.; Fan, Z. Efficient Activators for an Iron Catalyst in the Polymerization of Ethylene. *Macromol. Rapid Commun.* **2002**, *23*, 639–642. [CrossRef]

80. Bryliakov, K.P.; Talsi, E.P.; Semikolenova, N.V.; Zakharov, V.A. Formation and Nature of the Active Sites in Bis (imino) Pyridine Iron-based Polymerization Catalysts. *Organpmetallics* **2009**, *28*, 3225–3232. [CrossRef]

81. Hirvi, J.T.; Bochmann, M.; Severn, J.R.; Linnolahti, M. Formation of Octameric Methylaluminoxanes by Hydrolysis of Trimethyla-luminum and the Mechanisms of Catalyst Activation in Single-Site Olefin Polymerization Catalysis. *Chem. Phys. Chem.* **2014**, *15*, 2732–2742. [CrossRef] [PubMed]

82. Semikolenova, N.V.; Sun, W.-H.; Soshnikov, I.E.; Matsko, M.A.; Kolesova, O.V.; Zakharov, V.A.; Bryliakov, K.P. Origin of "Multisite-like" Ethylene Polymerization Behavior of the Single-Site Nonsymmetrical Bis(Imino)Pyridine Iron(II) Complex in the Presence of Modified Methylaluminoxane. *ACS Catal.* **2017**, *7*, 2868–2877. [CrossRef]

83. Boudene, Z.; Boudier, A.; Breuil, P.A.R.; Olivier-Bourbigou, H.; Raybaud, P.; Toulhoat, H.; de Bruin, T. Understanding the Role of Aluminum-Based Activators in Single Site Iron Catalysts for Ethylene Oligomerization. *J. Catal.* **2014**, *317*, 153–157. [CrossRef]

84. Ghiotto, F.; Pateraki, C.; Tanskanen, J.; Severn, J.R.; Lohmann, N.; Kusmin, A.; Stellbrink, J.; Linnolahti, M.; Bochmann, M. Probing the Structure of Methylalumoxane (MAO) by a Combined Chemical, Spectroscopic, Neutron Scattering, and Computational Approach. *Organometallics* **2013**, *32*, 3354–3362. [CrossRef]

85. Luo, L.; Sangokoya, S.A.; Wu, X.; Diefenbach, S.P.; Kneale, B. Aluminoxane Catalyst Activators Derived from Dialkylaluminum Cation Precursor Agents, Processes for Making Same, and Use Thereof in Catalysts and Polymerization of Olefins. WO 2009029857, 5 March 2009.

86. Marques, M.M.V.; Nunes, C.P.; Tait, P.J.T.; Dias, A.R. Polymerization of Ethylene Using a High-Activity Ziegler–Natta Catalyst. II. Molecular Weight Regulation. *J. Polym. Sci. A* **1993**, *31*, 219–225. [CrossRef]

87. Han, C.J.; Lee, M.S.; Byun, D.J.; Kim, S.Y. Synthesis of Hydroxy-Terminated Polyethylene via Controlled Chain Transfer Reaction and Poly(ethylene-b-caprolactone) Block Copolymer. *Macromolecules* **2002**, *35*, 8923–8925. [CrossRef]

88. Kretschmer, W.P.; Meetsma, A.; Hessen, B.; Schmalz, T.; Qayyum, S.; Kempe, R. Reversible Chain Transfer between Organoyttrium Cations and Aluminum: Synthesis of Aluminum-Terminated Polyethylene with Extremely Narrow Molecular-Weight. *Chem. Eur. J.* **2006**, *12*, 8969. [CrossRef] [PubMed]

89. Bochmann, M. The chemistry of catalyst activation: The Case of Group 4 Polymerization Catalysts. *Organometallics* **2010**, *29*, 4711. [CrossRef]

90. Britovsek, G.J.P.; Cohen, S.A.; Gibson, V.C.; Van Meurs, V.C. Iron Catalyzed Polyethylene Chain Growth on Zinc: A Study of the Factors Delineating Chain Transfer versus Catalyzed Chain Growth in Zinc and Related Metal Alkyl Systems. *J. Am. Chem. Soc.* **2004**, *126*, 10701. [CrossRef]

91. Meyer, R. Herstellung von Maßgeschneidertem Terminal-funktionalisiertem Polyethylen Mittels der Katalysierten Aufbaureak-tion. Ph.D. Thesis, Universität Hamburg, Hamburg, Germany, 2013.

92. Velthoen, E.Z.M.; Muñoz-Murillo, A.; Bouhmadi, A.; Cecius, M.; Diefenbach, S.; Weckhuysen, B.M. The Multifaceted Role of Methylaluminoxane in Metallocene-based Olefin Polymerization Catalysis. *Macromolecules* **2018**, *51*, 343–355. [CrossRef] [PubMed]

93. Zijlstra, H.S.; Harder, S. Methylalumoxane-History, Production, Properties, and Applications. *Eur. J. Inorg. Chem.* **2015**, *2015*, 19–43. [CrossRef]

94. Busico, V.; Cipullo, R.; Cutillo, F.; Friederichs, N.; Ronca, S.; Wang, B. Improving the Performance of Methylalumoxane: A Facile and Efficient Method to Trap "Free" Trimethylaluminum. *J. Am. Chem. Soc.* **2003**, *125*, 12402–12403. [CrossRef] [PubMed]

95. Li, Z.; Ma, Y.; Sun, W.H. Comparison of the Reactivity and Structures for the Neutral and Cationic Bis (imino) pyridyl Iron and Cobalt Species by DFT Calculations. *Catalysts* **2020**, *10*, 1396. [CrossRef]

96. Castro, P.M.; Lahtinen, P.; Axenov, K.; Viidanoja, J.; Kotiaho, T.; Leskelä, M.; Repo, T. Activation of 2, 6-bis (imino) Pyridine Iron (II) Chloride Complexes by Methyl aluminoxane: An Electrospray Ionization Tandem Mass Spectrometry Investigation. *Organometallics* **2005**, *24*, 3664–3670. [CrossRef]

97. Scott, J.; Gambarotta, S.; Korobkov, I.; Knijnenburg, Q.; de Bruin, B.; Budzelaar, P.H.M. Formation of a Paramagnetic Al Complex and Extrusion of Fe during the Reaction of (Diiminepyridine)Fe with AlR$_3$ (R = Me, Et). *J. Am. Chem. Soc.* **2005**, *127*, 17204–17206. [CrossRef] [PubMed]

98. Cam, D.; Giannini, U. Concerning the Reaction of Zirconocene Dichloride and Methylaluminoxane: Homogeneous Ziegler-Natta Catalytic System for Olefin Polymerization. *Macromol. Chem.* **1992**, *193*, 1049–1055. [CrossRef]

99. Kaminsky, W. The Discovery of Metallocene Catalysts and their Present State of the Art. *J. Polym. Sci. Part A Polym.* **2004**, *42*, 3911–3921. [CrossRef]

100. Elschenbroich, C.; Hensel, F.H.; Hopf, H. *Organometallchemie*, 6th ed.; Teubner Verlag: Wiesbaden, Germany, 2008; pp. 668–669.

101. Smit, T.M.; Tomov, A.K.; Britovsek, G.J.P.; Gibson, V.C.; White, A.J.P.; Williams, D.J. The Effect of Imine-Carbon Substituents in Bis (imino) Pyridine-Based Ethylene Polymerisation Catalysts across the Transition Series. *Catal. Sci. Technol.* **2012**, *2*, 643–646. [CrossRef]

102. Meyer, R.S.A.; Scholtyssek, J.S.; Luinstra, G.A. Facile Synthesis of Hydroxyl-Terminated Oligoethylenes. *Macromol. Mater. Eng.* **2015**, *300*, 218–225. [CrossRef]

103. Ziegler, K.; Kroll, W.-R.; Larbig, W.; Steudel, O.-W. Metallorganische Verbindungen, XXXII Zerfalls- und Austauschreaktionen der Aluminiumtrialkyle. *Liebigs Ann. Chem.* **1960**, *629*, 53–89. [CrossRef]

104. Ziegler, K.; Krupp, F.; Zosel, K. Metallorganische Verbindungen XL Synthese von Alkoholen aus Organoaluminium-Verbindungen. *Liebigs Ann. Chem.* **1960**, *629*, 241. [CrossRef]

105. Lundeen, A.J.; Yates, J.E. Primary Aliphatic Alcohol Preparation by Oxidation of Trialkylaluminum Compounds and Hydrolysis of the Products. GB 1144390, 5 March 1969.

106. Cossée, P. Ziegler-Natta Catalysis, I. Mechanism of Polymerization of α-Olefins with Ziegler-Natta Catalysts. *J. Catal.* **1964**, *3*, 80–88. [CrossRef]

107. Kissin, Y.V.; Qian, C.; Xie, G.; Chen, Y. Multi-center Nature of Ethylene Polymerization Catalysts Based on 2,6-Bis(imino)pyridyl Complexes of Iron and Cobalt. *J. Polym. Sci. A Polym. Chem.* **2006**, *44*, 6150–6170. [CrossRef]

108. Schmidt, R.; Welch, M.B.; Palackal, S.J.; Alt, H.G. Heterogenized Iron (II) Complexes as Highly Active Ethene Polymerization Catalysts. *J. Mol. Catal. A Chem.* **2002**, *179*, 155–173. [CrossRef]

109. Bianchini, C.; Mantovani, G.; Meli, A.; Migliacci, F.; Zanobini, F.; Laschi, F.; Sommazzi, A. Oligomerisation of Ethylene to Linear α-Olefins by new Cs- and C1-Symmetric [2,6-Bis(imino)pyridyl]iron and -cobalt Dichloride Complexes. *Eur. J. Inorg. Chem.* **2003**, *2003*, 1620–1631. [CrossRef]

110. Schmidt, R.; Welch, M.B.; Knudsen, R.D.; Gottfried, S.; Alt, H.G. N, N, N-Tridentate Iron (II) and Vanadium (III) Complexes: Part I. Synthesis and Characterization. *J. Mol. Catal. A Chem.* **2004**, *222*, 9–15.

111. Schmidt, R.; Welch, M.B.; Knudsen, R.D.; Gottfried, S.; Alt, H.G. N, N, N-Tridentate Iron (II) and Vanadium (III) Complexes: Part II: Catalytic Behavior for the Oligomerization and Polymerization of Ethene and Characterization of the Resulting Products. *J. Mol. Catal. A Chem.* **2004**, *222*, 17–25.

112. Zhang, W.; Jiang, B.B.; Ye, J.; Liao, Z.W.; Huang, Z.L.; Wang, J.D.; Yang, Y.R. Preparation of Aryloxy-aluminoxanes and Their Use as Activators in the Bis(imino)pyridyl Iron-catalyzed Oligomerization of Ethylene. *Chin. J. Polym. Sci.* **2018**, *36*, 1207–1216. [CrossRef]

113. Luinstra, G.A.; Werne, G.; Rief, U.; Kristen, M.O.; Queisser, J.A.; Geprägs, M. Transition Metal Complexes with Tridentate Ligands and Their Use as Catalysts in Manufacture of Olefin (co)Polymers. WO 2001007491 A1 20010201, 1 February 2001.

114. Barabanov, A.A.; Bukatov, G.D.; Zakharov, V.A.; Semikolenova, N.V.; Echevskaja, L.G.; Matsko, M.A. Kinetic Peculiarities of Ethylene Polymerization over Homogeneous Bis(imino)pyridine Fe(II) Catalysts with Different Activators. *Macromol. Chem. Phys.* **2005**, *206*, 2292–2298. [CrossRef]

115. Wang, Q.; Li, L.D.; Fan, Z.Q. Effects of Tetraalkylaluminoxane Activators on Ethylene Polymerization Catalyzed by Ironbased Complexes. *Eur. Polym. J.* **2005**, *41*, 1170–1176. [CrossRef]

116. Radhakrishnan, K.; Cramail, H.; Deffieux, A.; François, P.; Momtaz, A. Influence of Alkylaluminium Activators and Mixtures Thereof on Ethylene Polymerization with a Tridentate Bis(Imino)-Pyridinyliron Complex. *Macromol. Rapid Commun.* **2003**, *24*, 251–254. [CrossRef]

117. Britovsek, G.J.; Cohen, S.A.; Gibson, V.C.; Maddox, P.J.; van Meurs, M. Iron-Catalyzed Polyethylene Chain Growth on Zinc: Linear α-Olefins with a Poisson Distribution. *Angew. Chem. Int. Ed.* **2002**, *41*, 489–491. [CrossRef]

118. Van Meurs, M.; Britovsek, G.J.; Gibson, V.C.; Cohen, S.A. Polyethylene Chain Growth on Zinc Catalyzed by Olefin Polymerization Catalysts: A Comparative Investigation of Highly Active Catalyst Systems across the Transition Series. *J. Am. Chem. Soc.* **2005**, *127*, 9913–9923. [CrossRef] [PubMed]

119. Meyer, R.S.A.; Luinstra, G.A. Iron Catalyst in the Preparation of Polyolefin Composites. In *Polyolefins: 50 Years after Ziegler and Natta II. Advances in Polymer Science*; Kaminsky, W., Ed.; Springer: Berlin/Heidelberg, Germany, 2013; Volume 258, pp. 341–362.

120. Knijnenburg, Q.; Smits, J.M.M.; Budzelaa, P.H.M. Reaction of the Diimine Pyridine Ligand with Aluminum Alkyls: An Unexpectedly Complex Reaction. *Organometallics* **2006**, *25*, 1036–1046. [CrossRef]

121. Dedeutour, J.N.; Radhakrishnan, K.; Cramail, H.; Deffieux, A. Reactivity of Metallocene Catalysts for Olefin Polymerization: Influence of Activator Nature and Structure. *Macromol. Rapid Commun.* **2001**, *22*, 1095. [CrossRef]

122. Wang, Q.; Yang, H.X.; Fan, Z.Q.; Xu, H. Performance of Various Activators in Ethylene Polymerization Based on an Iron(II) Catalyst System. *J. Polym. Sci. Part A Polym. Chem.* **2004**, *42*, 1093–1099. [CrossRef]

123. Boudier, A.; Breuil, P.A.R.; Magna, L.; Olivier-Bourbigou, H.; Braunstein, P. Alternative Aluminum-Based Cocatalysts for the Iron-Catalyzed Oligomerization of Ethylene. *Dalton Trans.* **2015**, *44*, 12995–12998. [CrossRef]

124. Talsi, E.P.; Babushkin, D.E.; Semikolenova, N.V.; Zudin, V.N.; Panchenko, V.N.; Zakharov, V.A. Polymerization of Ethylene Catalyzed by Iron Complex Bearing 2,6-Bis(imine)pyridyl Ligand: ^{1}H and ^{2}H NMR Monitoring of Ferrous Species Formed via Catalyst Activation with AlMe$_3$, MAO, AlMe$_3$/B(C$_6$F$_5$)$_3$ and AlMe$_3$/CPh$_3$(C$_6$F$_5$)$_4$. *Macromol. Chem. Phys.* **2001**, *202*, 2046–2051. [CrossRef]

125. Chien, J.C.W.; Wang, B.P. Metallocene-Methylaluminoxane Catalysts for Olefin Polymerization. I. Trimethylaluminum as Coactivator. *J. Polym. Sci. Part A Polym. Chem.* **1988**, *26*, 3089. [CrossRef]

126. Khrushch, N.E.; Bravaya, N.M. Interaction of Zirconocenes with Polymethyl alumoxane. Kinetics of Methane Liberation. *J. Mol. Cat. A Chem.* **2000**, *156*, 69. [CrossRef]

127. Ystenes, M. The Trigger Mechanism for Polymerization of α-Olefins with Ziegler-Natta Catalysts: A New Model Based on Interaction of Two Monomers at the Transition State and Monomer Activation of the Catalytic Centers. *J. Catal.* **1991**, *129*, 383–401. [CrossRef]

128. Resconi, L.; Bossi, S.; Abis, L. Study on the Role of Methylaluminoxane in Homogeneous Olefin Polymerization. *Macromolecules* **1990**, *23*, 4489. [CrossRef]

129. Barabanov, A.A.; Semikolenova, N.V.; Mats'ko, M.A.; Zakharov, V.A. Kinetic Regularities of Catalytic Ethylene Polymerization on Single- and Multi-Site Cobalt and Vanadium Bis(imino)pyridine Complexes. *Kinet. Catal.* **2013**, *54*, 475–480. [CrossRef]

130. Scholtyssek, J. Entwicklung einer Dreistufigen in-situ Synthese von Polyethylen/Silica-Nanocomposites. Ph.D. Thesis, Universität Hamburg, Hamburg, Germany, 2012.

131. Small, B.L.; Brookhart, M. Polymerization of Propylene by a New Generation of Iron Catalysts: Mechanisms of Chain Initiation, Propagation, and Termination. *Macromolecules* **1999**, *32*, 2120–2130. [CrossRef]

132. Wagner, H.L. The Mark–Houwink–Sakurada Equation for the Viscosity of Linear Polyethylene. *J. Phys. Chem. Ref. Data* **1985**, *14*, 611. [CrossRef]